RecA bundles mediate homology pairing between distant sisters during *Escherichia coli* DNA break repair

Christian Lesterlin, Graeme Ball, Lothar Schermelleh and David J. Sherratt

Department of Biochemistry, University of Oxford, Oxford, OX1 3QU, UK

Corresponding author: david.sherratt@bioch.ox.ac.uk

Running Head: *E. coli DSB repair in vivo*

Keywords: *Escherichia coli* / homologous recombination / double-strand break repair / chromosome segregation/ super resolution microscopy

Double-strand break (DSB) repair by homologous recombination (HR) has evolved to maintain genetic integrity in all organisms[1]. Although many reactions that occur during HR are known[1-3], understanding of where, when and how they occur in cells is lacking. By using conventional and super-resolution microscopy we describe the progression of DSB repair in live *Escherichia coli*. Specifically, we address whether HR can occur efficiently between distant sister loci that have segregated to opposite halves of an *E. coli* cell. We show that a site-specific DSB in one sister can be repaired efficiently using distant sister homology. After RecBCD processing of the DSB, RecA is recruited to the cut locus, where it nucleates into a bundle that contains many more RecA molecules than can associate with the two ssDNA regions that form at the DSB. Mature bundles extend along the cell long axis in the space between the bulk nucleoid and the inner membrane. Bundle formation is followed by pairing in which the two ends of the cut locus relocate at the periphery of the nucleoid and together move rapidly towards the homology of the uncut sister. After sister locus pairing, RecA bundles disassemble and proteins that act late in HR are recruited to give viable recombinants 1-2 generation time equivalents after formation of the initial DSB. Mutated RecA proteins that do not form bundles are defective in sister pairing and in DSB-induced repair. The work reveals an unanticipated role of RecA bundles in channeling the movement of the DNA DSB ends, thereby facilitating the long-range homology search that occurs prior to the strand invasion and transfer reactions.

Although repair of DSBs by HR is efficient in *E. coli*, it is not known whether HR events are restricted to the ~15 min period in which sister loci remain in close association after replication[4,5], or whether HR can occur between distant segregated sister loci (~1.3 μm apart). To test whether segregated distant sisters can undergo recombination when a site-specific DSB was introduced into one sister, ~1 Mbp from the replication *oriC*, we expressed small amounts of unstable I-SceI endonuclease[6], so that most cells had only one of two sisters cleaved, and repaired the DSB efficiently in reactions that required RecABCD (Fig. 1 and Extended Data Fig. 1).

Fluorescent ParB-protein binding to DNA on either side of the cut site allowed us

to monitor the fate of cut and uncut loci. After DSB induction, loss and randomized positioning of foci occurred, when compared to the uncut control, in which 1-focus cells had the focus displaced slightly from midcell and 2-focus cells had the foci on either side of midcell. Time-lapse analysis showed focus pairing, accompanied by increased fluorescence, and focus-loss, dependent on RecBCD degradation; events absent in wild-type cells (Fig. 1a, c and Extended Data Fig. 1a, 2). RecABCD-dependent sister pairing occurred on average ~100 min after induction of I-SceI expression and persisted for ~50 min before sister re-segregation (Fig. 1a). The two ends of the DSB remained in proximity after cutting and during subsequent processing, supporting schemes in which both DNA ends are engaged in HR repair (Fig. 1c and Extended Data Fig. 2a), as reported for eukaryotic repair[7]. The behavior of fluorescent foci marking each of the cut ends was similar, with the foci moving to the cell periphery after cutting (compare Fig. 1a and Extended Data Fig. 1d; Fig. 1b). RecBCD processing of the DSB was bidirectional consistent with efficient loading of RecBCD complexes onto both ends of the break. The rate of DNA degradation in the absence of RecA was ~190 bp/s per RecBCD complex, eventually leading to complete nucleoid degradation (Fig. 1c, d and Extended Data Fig. 2b, c; Video S1; Supplementary discussion).

RecBCD-dependent recruitment of RecA to the DSB was assayed in cells expressing a C-terminal fusion of RecA to green fluorescent protein (GFP)[8] and wild-type RecA, both expressed from wild-type chromosomal *recA* promoters. These cells exhibited wild-type repair and recombination, whereas those expressing RecA-GFP alone were not fully repair-proficient (Extended Data Fig. 3a)[8]. Prior to DSB-induction, ~95% of cells showed RecA-GFP fluorescence uniformly distributed throughout the cell, with ~5% of cells having fluorescent spots that were not associated with a marked locus (21% colocalization) (Extended Data Fig. 3b). After DSB induction, fluorescent RecA spots appeared close to or coincident with one of the two marked sister loci (64% colocalization; Fig. 2a). The transient RecA spots nucleated rapidly into filamentous structures that we term RecA-bundles, which had formed their maximum length by ~13 min and most often extended along the cell (Fig. 2b; Video S2). The DSB-induced stimulation of RecA spot and bundle formation required RecBCD processing of the cut ends (Fig. 2c).

Rapid sister locus pairing occurred ~47 min after RecA bundle formation (Fig. 2d). During this period, no consistent changes in bundle architecture occurred and no significant turnover of RecA within the mature bundle structure was observed by FRAP (Fluorescence Recovery After Photobleaching; Extended Data Fig. 3c; Video S3). Once initiated, sister focus pairing was rapid (within 5 min in 69% of events) and was asymmetric with the cut sister traveling ~84% of the ~1.3 μm distance between sister loci (Fig. 2e, g). Although the cut and uncut loci showed similar diffusion coefficients (D_{app}), the movement of the cut locus was 5-7-fold more directional than the uncut locus, indicative of channeling of the movement of the cut locus (Extended Data Fig. 4a).

We propose that nucleation of RecA onto the ssDNA ends formed by RecBCD processing at the DSB triggers polymerization of RecA into bundles, which are required for pairing between distant sisters. RecA bundles disassembled rapidly and unidirectionally ~17 min after pairing of the sister loci, possibly triggered by the loss of the ssDNA-RecA ends upon strand invasion (Fig. 2f; Video S2). After pairing, sisters re-segregated and cells re-established normal growth, cell division and chromosome segregation. In parallel, we have shown that DSB-induction and bundle formation are followed by the recruitment of PriA and RecG recombination proteins that promote replication restart and recombination intermediate processing. In contrast, RecN was recruited early to the break (Extended Data Fig. 4b and c; Supplementary Discussion). Bundles of wild-type RecA that formed in response to DSBs were also observed in fixed cells using immunocytochemistry and in live cells with a more functional RecA803-RFP fusion (Extended Data Fig. 5)[9]. Furthermore, repair-deficient cells expressing RecAK72A-GFP, which fails to bind ATP, did not form spots or bundles, whereas cells expressing RecAK72R-GFP, which binds ATP but is hydrolysis impaired[10], formed weak spots close to the cut locus (0.49 ±0.2 μm), consistent with RecAK72R forming filaments on ssDNA and initiating strand transfer *in vitro*[10]. Nevertheless, the RecAK72R-GFP spots failed to nucleate bundles, and *recAK72R* cells did not show sister pairing and were repair-deficient (Extended Data Fig. 5). These data demonstrate that RecA bundles are physiologically relevant forms of RecA that are critical for HR repair between distant regions of homology.

To gain more insight into RecA bundle architecture and function, we used super-

resolution 3D-structured illumination microscopy (3D-SIM) and live cell time-lapse imaging (Fig. 3). RecA-bundles most frequently adopted overall longitudinal trajectories, with some radial writhing (Video S4) and were located between the surface of the nucleoid and the inner membrane. Bundles may be excluded from the nucleoid because of their size, as are ~20 nm diameter ribosomes[11], and their localization at the cell membrane could arise because activated forms of RecA may associate with phospholipid membranes[12]. 3D-SIM showed that 91% of bundles were associated with at least one sister focus, confirming the earlier data (Fig. 3a; Extended Data Fig. 3b; Video S5). Bundles were on average ~1.4 μm long and typically consisted of a ~160 nm thick central region bounded by thinner (≤100 nm) extensions (Extended Data Fig. 3b). 3D SIM-time-lapse analysis revealed that the central region was relatively immobile whereas the thin extensions moved rapidly and appeared to probe the inner cell compartment (Fig. 3a; Video S6-7).

Bundles contained ~70% of the normal pool of cellular RecA, estimated to be ~4640 ±1908 molecules/cell, independently of the presence of spots or bundles (Fig. 3b, c and Extended Data Fig 3d; Supplementary Discussion). The rate of RecA incorporation into DSB-induced bundles was ~4 monomer/s, which compares with an *in vitro* rate of 0.5-7 monomer/s/DNA end, or nucleation point[13,14]. We estimate that >85 % of RecA molecules present in bundles are likely to be DNA-free and additional to the two presynaptic ssDNA-RecA filaments that we propose nucleate bundle formation (Supplementary Discussion). DNA-free RecA filaments and bundles can form *in vitro*[15,16], and have a similar architecture to that of RecA-DNA filaments[17-19]. The observed ~1.4μm length of RecA bundles is less than the ~2.5 μm long twin filament that would form from ~3200 RecA molecules nucleating onto the two ssDNA ends at the break. Thus, RecA bundles may contain lateral filaments, potentially explaining the thicker central regions of the bundles. RecA bundles have been observed in previous light microscopy and EM studies, and have been shown to appear in response to DNA damage in *E. coli*[8,20,21], and in response to DSBs in *Bacillus subtilis*[22]. In the later case spots appeared close to the site of the DSB and extended into longitudinal bundles, whose formation was dependent on the *B. subtilis* RecBCD orthologue, AddAB. Nevertheless, their physiological significance has been unclear, though it was proposed that RecA

bundles are inactive storage forms[8,18].

Our data demonstrate conclusively that DSB-induced homology pairing can occur between distant segregated sister loci, and therefore HR is not restricted to the ~15 min cohesion period following replication. We propose that RecA bundles, actively facilitate the process of locus pairing between distant sisters, thereby leading to the eventual homology-directed strand invasion. The observation that sister pairing is not necessarily accompanied by bundle shortening suggests that the DNA ends move along the bundle. This could be driven by sliding between RecA filaments within the bundle as proposed for ParM-mediated DNA movement[23], a treadmilling mechanism in which RecA filament growth at the leading edge and disassembly in the region of the cut locus could lead to rapid pairing, or a process in which a motor-like protein associated with the cut ends moves along the bundle, akin to other motor proteins moving along cytoskeletal elements. Mechanisms in which pairing arises in part as 'passive' 1D diffusion along a restraining bundle, would still require a process that directs the cut locus towards the opposite side of the cell. In any of these scenarios, the channeled movement of the cut ends would be 'blind' to the uncut sister until a local homology search accompanied by strand invasion generated the strand transfer complex whose processing leads to completed recombination products. It follows therefore that nucleation of a RecA spot into a bundle should occur irrespective of whether sister homology is present. Consistent with this, RecA bundles formed at similar frequencies regardless of whether sister homology was present (Extended Data Fig. 3e; Supplementary Discussion). The two–step mechanism we propose only needs to be used when sister homology is distant from the cut locus; immediately after replication, when sister loci remain in close proximity, DSB repair by HR might occur simply by the canonical mechanism of strand invasion and transfer.

The formation of RecA bundles and equivalent structures in other organisms may be a general mechanism for channeling the movement of damaged DNA loci, thereby enabling a genome-wide homology search in a cell compartment at the periphery of the nucleoid. Since other repair proteins are known to interact with RecA and its orthologues, bundles may promote the binding and movement of other players in DNA repair. In eukaryotes, HR may also fall into two classes defined by the distance the homology

search needs to take. For example, allelic events between cohesed sisters and between paired homologues in meiosis do not involve distant pairing events. In contrast, non-allelic HR events, or those between homologous mitotic chromosomes may use processes that involve the equivalent of RecA bundles to facilitate the homology search, a process that may take longer, as observed for inter-homologue HR intermediates[7].

METHODS SUMMARY

Bacteria were derivatives of *E. coli* K12 TB28 (MG1655, *ΔlacIZYA*). Mutations were introduced by λ-Red recombination or P1 transduction. Cells were grown at 30°C in M9 0.2% glucose and antibiotics when required. Exponentially growing cells (A_{600} 0.1-0.2) were used for microscopy. Full details of bacteria and plasmids used, as well as protocols for sample preparation, imaging and analyses can be found in Supplementary Information.

REFERENCES

1 Cromie, G. A., Connelly, J. C. & Leach, D. R. Recombination at double-strand breaks and DNA ends: conserved mechanisms from phage to humans. *Mol Cell* **8**, 1163-1174 (2001).

2 Cox, M. M. Regulation of bacterial RecA protein function. *Critical reviews in biochemistry and molecular biology* **42**, 41-63, doi:10.1080/10409230701260258 (2007).

3 Dillingham, M. S. & Kowalczykowski, S. C. RecBCD enzyme and the repair of double-stranded DNA breaks. *Microbiol Mol Biol Rev* **72**, 642-671, Table of Contents, doi:10.1128/MMBR.00020-08 (2008).

4 Lesterlin, C., Gigant, E., Boccard, F. & Espeli, O. Sister chromatid interactions in bacteria revealed by a site-specific recombination assay. *Embo J* **31**, 3468-3479, doi:emboj2012194 [pii]10.1038/emboj.2012.194 (2012).

5 Reyes-Lamothe, R., Possoz, C., Danilova, O. & Sherratt, D. J. Independent positioning and action of Escherichia coli replisomes in live cells. *Cell* **133**, 90-102, doi:10.1016/j.cell.2008.01.044 (2008).

6 Monteilhet, C., Perrin, A., Thierry, A., Colleaux, L. & Dujon, B. Purification and characterization of the in vitro activity of I-Sce I, a novel and highly specific endonuclease encoded by a group I intron. *Nucleic Acids Res* **18**, 1407-1413 (1990).

7 Bzymek, M., Thayer, N. H., Oh, S. D., Kleckner, N. & Hunter, N. Double Holliday junctions are intermediates of DNA break repair. *Nature* **464**, 937-941, doi:10.1038/nature08868 (2010).
8 Renzette, N. *et al.* Localization of RecA in Escherichia coli K-12 using RecA-GFP. *Mol Microbiol* **57**, 1074-1085, doi:10.1111/j.1365-2958.2005.04755.x (2005).
9 Handa, N., Amitani, I., Gumlaw, N., Sandler, S. J. & Kowalczykowski, S. C. Single molecule analysis of a red fluorescent RecA protein reveals a defect in nucleoprotein filament nucleation that relates to its reduced biological functions. *J Biol Chem* **284**, 18664-18673, doi:10.1074/jbc.M109.004895 (2009).
10 Rehrauer, W. M. & Kowalczykowski, S. C. Alteration of the nucleoside triphosphate (NTP) catalytic domain within Escherichia coli recA protein attenuates NTP hydrolysis but not joint molecule formation. *J Biol Chem* **268**, 1292-1297 (1993).
11 Bakshi, S., Siryaporn, A., Goulian, M. & Weisshaar, J. C. Superresolution imaging of ribosomes and RNA polymerase in live Escherichia coli cells. *Mol Microbiol* **85**, 21-38, doi:10.1111/j.1365-2958.2012.08081.x (2012).
12 Garvey, N., St John, A. C. & Witkin, E. M. Evidence for RecA protein association with the cell membrane and for changes in the levels of major outer membrane proteins in SOS-induced Escherichia coli cells. *J Bacteriol* **163**, 870-876 (1985).
13 Bell, J. C., Plank, J. L., Dombrowski, C. C. & Kowalczykowski, S. C. Direct imaging of RecA nucleation and growth on single molecules of SSB-coated ssDNA. *Nature* **491**, 274-278, doi:10.1038/nature11598 (2012).
14 Feinstein, E. *et al.* Single-molecule studies of the stringency factors and rates governing the polymerization of RecA on double-stranded DNA. *Nucleic Acids Res* **39**, 3781-3791, doi:10.1093/nar/gkr013 (2011).
15 Brenner, S. L., Zlotnick, A. & Griffith, J. D. RecA protein self-assembly. Multiple discrete aggregation states. *J Mol Biol* **204**, 959-972. (1988).
16 DiCapua, E., Schnarr, M., Ruigrok, R. W., Lindner, P. & Timmins, P. A. Complexes of RecA protein in solution. A study by small angle neutron scattering. *J Mol Biol* **214**, 557-570, doi:10.1016/0022-2836(90)90198-U (1990).
17 Chen, Z., Yang, H. & Pavletich, N. P. Mechanism of homologous recombination from the RecA-ssDNA/dsDNA structures. *Nature* **453**, 489-484, doi:10.1038/nature06971 (2008).
18 Story, R. M., Weber, I. T. & Steitz, T. A. The structure of the E. coli recA protein monomer and polymer. *Nature* **355**, 318-325, doi:10.1038/355318a0 (1992).
19 Yu, X., VanLoock, M. S., Yang, S., Reese, J. T. & Egelman, E. H. What is the structure of the RecA-DNA filament? *Current protein & peptide science* **5**, 73-79 (2004).
20 Levin-Zaidman, S. *et al.* Ordered intracellular RecA-DNA assemblies: a potential site of in vivo RecA-mediated activities. *Proc Natl Acad Sci U S A* **97**, 6791-6796, doi:10.1073/pnas.090532397 (2000).

21 Renzette, N. & Sandler, S. J. Requirements for ATP binding and hydrolysis in RecA function in Escherichia coli. *Mol Microbiol* **67**, 1347-1359, doi:10.1111/j.1365-2958.2008.06130.x (2008).
22 Kidane, D. & Graumann, P. L. Dynamic formation of RecA filaments at DNA double strand break repair centers in live cells. *The Journal of cell biology* **170**, 357-366, doi:10.1083/jcb.200412090 (2005).
23 Gayathri, P. *et al.* A bipolar spindle of antiparallel ParM filaments drives bacterial plasmid segregation. *Science* **338**, 1334-1337, doi:10.1126/science.1229091 (2012).

SUPPLEMENTARY INFORMATION is available in the online version of the paper.

ACKNOWLEDGEMENTS

The work was supported by an EMBO Long-term fellowship to CL (LTF-535-2009); to a Wellcome Trust Programme Grant to DJS (WT083469MA) and by a Wellcome Trust Strategic Award (091911) supporting advanced microscopy at Micron Oxford (http://micronoxford.com). We thank Ian Dobbie for his generous support and advice on imaging. We thank David Leach and Stephen Kowalczykowski for the gift of strains and plasmids, Nelly Dubarry for critical reading of the manuscript and Mathieu Stouf for the gift of pMS11. We thank E. Birt and K. Prosser for preliminary experiments.

AUTHOR CONTRIBUTIONS

DJ.S and C.L conceived the project, interpreted the data and wrote the paper. C.L designed and undertook experiments. G.B. developed analytical tools for microscopy data and provided advice on the manuscript. L.S. provided expertise on 3D-SIM and advice on the manuscript.

AUTHOR INFORMATION

Author Information Reprints and permissions information is available at www.nature.com/reprints. Correspondence and requests for materials should be addressed to DJ.S. (david.sherratt@bioch.ox.ac.uk).

FIGURE LEGENDS

Figure 1. Effects of DSB-induction on positioning of adjacent chromosome loci.

(a) Schematic of DSB-induction. Snapshot analysis of DSe (Downstream end) localisation before (left) and after 60 min of DSB induction (right). ISD, mean Inter-Sister Distance. Bottom panel, time-lapse analysis (5 min/frame) of DSe focus dynamics.

(b). Distributions of DSe foci along the cell diameter before and after 60 min of DSB induction. Data are shown for cut sites that changed position after DSB induction.

(c). DSB-induced reduction of the fraction of cells with DSe and USe foci is RecBCD-dependent and indicates simultaneous processing of both DSB ends.

(d). DSe and USe foci remain coincident during sister pairing and subsequent sister separation.

Figure 2. RecA bundle formation and disassembly, and RecA-mediated sister locus pairing.

(a). RecA-GFP spot formation in relation to the cut locus during sister pairing using. wide-field microscopy. D, mean distance between the centres of RecA spots and the closest DSe focus .

(b). Wide-field imaging of nucleation of RecA bundles from RecA-GFP spots at DSe.

(c). Snapshot analysis of RecB-dependent RecA-GFP bundle formation as a function of DSB-induction time (500 cells analysed for each dataset).

(d). Timing of bundle formation and sister pairing (time-lapse analysis; n events).

(e). Mobility of sister loci during sister pairing. DSe focus positions over 300 s time-lapse (5 s/frame) during pairing, with corresponding kymograph. See Methods Online for definition and determination of directionality.

(f). RecA-GFP bundle disassembly shown by simultaneous time-lapse imaging of RecA-GFP and DSe and of RecA-GFP.

(g). Schematic of DSB-end and RecA dynamics during DSB repair by *E. coli* HR, based on integration of all data.

Figure 3. Super-resolution imaging of RecA bundles reveals their intracellular localization

(a). 3D-structured-illumination-microscopy (3D-SIM) of cells with DSB-induced RecA-GFP bundles alone (i), with DSe foci (ii), relative to DNA (iii), and to membrane (iv). (v), bundle architecture. (vi), the dynamic behavior of RecA bundle thin extensions is illustrated by the projection of the movement over 200s (taken from Video S7).

(b). Total fluorescence intensity distribution and average fluorescence of RecA-GFP in cells with or without bundles, and of MukB-GFP.

(c). The fraction of total cellular RecA monomers within bundles. See Online Methods. 70 ±18 % of the intracellular fluorescence was incorporated into bundles.

MATERIAL AND METHODS

Bacterial strains and growth

All strains are derivatives of *E. coli* K12 TB28 (MG1655, Δ*lacIZYA*[24]). Cells were grown at 30°C in M9 media supplemented with 0.2% glucose. Ampicillin (100 µg/ml), kanamycin (50 µg/ml), chloramphenicol (20 µg/ml) and tetracycline (10 µg/ml) were added when required. Expression of I-SceI endonuclease from an arabinose inducible promoter[25] was induced by the addition of 0.2% arabinose. Intracellular localisation of chromosomal loci flanking the *I-SceI*^{CS} cut site was visualized by fluorescent wide-field microscopy using two distinct ParB/*parS* systems[26]. Mutations were generally constructed by λ-Red recombination[27] and further introduced into the strain of interest by P1 transduction. When needed, the DNA region between the two *frt* sites (*cam/kan* resistance genes) was removed using Flp recombinase expressed from pCP20[27].

Microscopy sample preparation

All microscopy experiments were performed on live cells growing in exponential phase (A_{600}~0.1-0.2). Cells were transferred from liquid culture to a slide mounted with 1% agarose in M9 glucose 0.2% medium and incubated during microscopy at the required temperature using an incubation chamber. 3D-structured illumination microscopy (3D-SIM) snapshots were performed at 24 ºC with cells covered with precision cover glass thickness No. 1.5H (tol. ±5 µm; Marienfeld Superior) using immersion oil with 1.512 refractive index. For time-lapses after DSB induction, arabinose 0.2% was added to the liquid culture for 30 min before the cell were mounted on the slide. Nucleoids were visualized using 4 µg/ml 4',6-diamidino-2-phenylindole (DAPI), and cells membrane were visualized using 1 µg/ml FM4-64 (Life Technologies).

Wide-field microscopy, 3D-structured illumination microscopy and FRAP imaging

Conventional wide-field fluorescence microscopy was carried out on an Eclipse TE2000-U microscope (Nikon), equipped with a 100x/1.4 oil PlanApo objective and either a

Cool-Snap HQ CCD or a QuantEM camera (Photometrics), and using Metamorph software for image acquisition. Super-resolution 3D-SIM imaging as well as conventional wide-field imaging was performed on a DeltaVision OMX V3 (Applied Precision/GE Healthcare) equipped with a Blaze SIM module, a 60x/1.42 oil UPlanSApo objective (Olympus), 405 nm and 488 nm and 593 nm diode lasers and three sCMOS cameras (PCO). The fast-live mode enabled ultra-high speed illumination and simultaneous or sequential acquisition of multiple-color 3D stacks of RecA-GFP/DAPI, RecA-GFP/FM4-64, RecA-GFP/mCherry or RecA-GFP alone. For each color, the raw 3D-SIM stacks were composed of 225 images (512×512 pixels) consisting of 15 z-sections (125 nm z-distance, sample thickness of 1.750 µm), with 15 images per z-section with the striped illumination pattern [28,29] rotated to the three angles (-60°, 0°, +60°) and shifted in five phase steps. Acquisition settings were as follows: RecA-GFP, 2-5 ms exposure with 488 nm laser (attenuated to 10% transmission); DAPI, 20 ms exposure with 405 nm laser (100% transmission); FM4-64, 30 ms exposure with 593 nm laser (100% transmission). Total acquisition times per stack were 1.8 s for RecA-GFP, and ~10 s for RecA-GFP/DAPI and RecA-GFP/FM4-64. Note that simultaneous imaging of RecA-GFP and DSe (ParB-mCherry) was performed in 3D-SIM mode for RecA-GFP and conventional wide-field for ParB-mCherry. The 3D-SIM raw data was computationally reconstructed with SoftWoRx 6.0 (Applied Precision) using Wiener filter settings 0.002 and channel specifically measured optical transfer functions to generate a super-resolution 3D image stack with a lateral (x-y) resolution of 100-130 nm (wavelength-dependent) and an axial (z) resolution of ~300 nm. In the reconstruction process the pixel size is halved from 80 nm to 40 nm and the pixel number doubled in order to meet the Nyquist sampling criterion. The number of pixels in the DSe conventional images were doubled using Priism (Image Visualization Environment, http://msg.ucsf.edu/IVE/) in order to merge with 3D-SIM images. A constrained iterative 3D image deconvolution was applied to conventional wide-field data in SoftWorX 6.0. Images from the different color channels were registered with alignment parameter obtained from calibration measurements with 0.2 µm diameter TetraSpeck beads (Life Technologies) using the OMX Editor software (Chris Weisiger & John Sedat, UCSF; unpublished). FRAP experiments were performed with an UltraVIEW VoX spinning disk

confocal system with Photokinesis module (PerkinElmer) assembled on an IX8 microscope (Olympus) equipped with an C9100-13 EMCCD camera (Hamamatsu) and a 100x/1.4 oil PlanApo objective (Olympus). Photobleaching of a small diffraction-limited spot was carried out with a focused 488 nm laser beam (100 ms with AOTF set to 50% transmission). Fluorescence intensity measurements of the unbleached and bleached regions were performed using ImageJ (rsbweb.nih.gov/ij/). Values were normalized to those of initial prebleaching images.

Snapshot and time-lapse analysis

Snapshot analysis was performed with the MicrobeTracker suite[30] extended by custom MATLAB routines which we specifically developed to generate focus positioning dotplots, histograms of 0/1/2-focus cell fractions, 2-color cell-type counting, inter-sister-focus distance (ISD), USe-DSe distance, focus position along the cell long X-axis (length) and short Y-axis (width). Distributions of DSe foci along the cell diameter presented Fig. 1b were performed by subdividing cells into five cell slices of equivalent areas as indicated in Meile *et al.,* (2011)[31]. Stoichiometry of RecA was determined by convolving the total fluorescence in *recA-GFP* cells and compare it to that of *mukB-GFP* cells for which MukB stoichiometry is known[32]. Total intracellular fluorescence intensity distribution analysis was performed on images resulting from the average projection of 15 z-sections (125 nm z-distance) corresponding to a sample thickness of 1.750 µm, using MicrobeTracker. Our estimate of RecA stoichiometry is in the range of previous estimates[33-36]. Fluorescent particle tracking during long time-lapses (>30 s/frame) was performed using a semi-automated custom MATLAB routine as previously described[37]. Mean Square Displacement (MSD) in X and Y dimensions and directionality of movement were obtained by running the View5D plug-in (ImageJ) on short time-lapses (300 s; 5 s/frame). The apparent 2D diffusion coefficient (D_{app}) was calculated from the initial slope of MSD plotted against time using $MSD_{XY}=4(D_{app})t$. The directionality of movement reflects the fraction of the overall displacement ($\Delta d_{1\text{-}t}$), compared to the total distance travelled by the focus ($\Delta d_1+\Delta d_2\ldots+\Delta d_t$) i.e., Directionality=($\Delta d_{1\text{-}t}/(\Delta d_1+\Delta d_2\ldots+\Delta d_t)$).

Immunocytochemistry

Cells were fixed in phosphate buffered saline with paraformaldehyde 5% (pH 7.2) and glutaraldehyde 0.06% and immobilized on poly-L-lysine slides (Poly-prep from Sigma-Aldrich), followed by treatment with lysozyme 1µg/ml. Immunocytochemistry was performed using rabbit anti-RecA polyclonal antibodies (Abnova), which were revealed using anti-rabbit secondary antibodies conjugated to Alexa 594 (Life Technologies). Coverslips were mounted with Vectashield mounting medium (Vector Laboratories).

Flow cytometry

Cells were grown in M9 glucose at 30ºC and sampled in late stationary phase, exponential phase (A_{600}~0.15) and 3 hours after incubation with cephalexin and rifampicin (run-out). Cell samples were prepared as described[38] except that Syto16 (Life Technologies) was used to stain DNA. Analysis was performed on FACScalibur flow cytometer (BD Biosciences). Data files were analyzed using CellQuest (BD Biosciences) and Weasel (WEHI; http://www.wehi.edu.au/).

Construction of I-SceI system for induction of site-specific DSB into the *E. coli* chromosome

The Rec^+ strain, in which DSB were initially induced corresponds to TB28 with both the *I-SceI* cut site and the gene encoding the *I-SceI* endonuclease inserted into *codA-cynR* and *araB* chromosome loci, respectively. The *I-SceI*^{CS} cassette carries *frt-cam-parSP1-frt-3*χ^+*-I-SceI*^{CS}*-parSPMT1-3*χ^- where *I-SceI*^{CS} stands for the cut site (5'-TAGGGATAACAGGGTAAT-3'), +/- stand for the orientation of 5'-GCTGGTGG-3' χ-sites[39] and *frt* indicates the Flp site-specific recombination sites. *parS* sites were amplified from pGBKD3-*parSPMT1* and pGBKD3-*parSP1* plasmids[40]. The cassette was integrated into *codA-cynR* intergenic region of MG1655 chromosome (356.6 kb) or into *ydeO-ydeP* intergenic region (1,581.7 kb) by λ-Red recombination[27] and further

transferred by P1 transduction into TB28. The wild-type allele of a *I-SceI* gene under the control of arabinose inducible promoter (carried by pDL2655 plasmid described in White *et al.,* (2008)[39]) was fused to 1X*c-Myc* tag followed by the DAS+4-degron tag in its C-terminus[41] amplified from pROD60. This plasmid carrying a 6-aa linker, Myc tag, 2-aa linker and the DAS+4 degron tag (S A G S A A E Q K L I S E E D L S S A A N D E N Y S E N Y A D A S) was as described[42]. The *I-SceI-degron* construct was tested for its reduced efficiency to linearize a *I-SceI*$_{CS}$-carrying plasmid after induction with 0.2% arabinose *in vivo*. P_{ara} *I-SceI-frt-kan* or P_{ara}*I-SceI-degron-frt-kan* constructs were inserted in the *araB* gene (70 kb) of MG1655/pKD46 by the process of λ-Red recombination and further transferred into TB28 by P1 transduction. The *recA* gene with its P_{recA} promoter region were amplified from K12 genomic DNA and subsequently integrated downstream of *fhuB* gene on MG1655 chromosome (171 kb on the chromosome) by λ-Red recombination and transferred into TB28 by P1 transduction (referred as *fhuB::recA-cat*).

REFERENCES

24 Bernhardt, T. G. & de Boer, P. A. Screening for synthetic lethal mutants in Escherichia coli and identification of EnvC (YibP) as a periplasmic septal ring factor with murein hydrolase activity. *Mol Microbiol* **52**, 1255-1269, doi:10.1111/j.1365-2958.2004.04063.x (2004).

25 Guzman, L. M., Belin, D., Carson, M. J. & Beckwith, J. Tight regulation, modulation, and high-level expression by vectors containing the arabinose PBAD promoter. *J Bacteriol* **177**, 4121-4130 (1995).

26 Nielsen, H. J., Ottesen, J. R., Youngren, B., Austin, S. J. & Hansen, F. G. The Escherichia coli chromosome is organized with the left and right chromosome arms in separate cell halves. *Mol Microbiol* **62**, 331-338, doi:10.1111/j.1365-2958.2006.05346.x (2006).

27 Datsenko, K. A. & Wanner, B. L. One-step inactivation of chromosomal genes in Escherichia coli K-12 using PCR products. *Proc Natl Acad Sci U S A* **97**, 6640-6645 (2000).

28 Gustafsson, M. G. *et al.* Three-dimensional resolution doubling in wide-field fluorescence microscopy by structured illumination. *Biophys J* **94**, 4957-4970, doi:10.1529/biophysj.107.120345 (2008).

29 Schermelleh, L. *et al.* Subdiffraction multicolor imaging of the nuclear periphery with 3D structured illumination microscopy. *Science* **320**, 1332-1336, doi:10.1126/science.1156947 (2008).

30 Sliusarenko, O., Heinritz, J., Emonet, T. & Jacobs-Wagner, C. High-throughput, subpixel precision analysis of bacterial morphogenesis and intracellular spatio-temporal dynamics. *Mol Microbiol* **80**, 612-627, doi:10.1111/j.1365-2958.2011.07579.x (2011).
31 Meile, J. C. *et al.* The terminal region of the E. coli chromosome localises at the periphery of the nucleoid. *BMC microbiology* **11**, 28, doi:10.1186/1471-2180-11-28 (2011).
32 Badrinarayanan, A., Reyes-Lamothe, R., Uphoff, S., Leake, M. C. & Sherratt, D. J. In vivo architecture and action of bacterial structural maintenance of chromosome proteins. *Science* **338**, 528-531, doi:10.1126/science.1227126 (2012).
33 Stohl, E. A. *et al.* Escherichia coli RecX inhibits RecA recombinase and coprotease activities in vitro and in vivo. *J Biol Chem* **278**, 2278-2285, doi:10.1074/jbc.M210496200 (2003).
34 Sommer, S., Boudsocq, F., Devoret, R. & Bailone, A. Specific RecA amino acid changes affect RecA-UmuD'C interaction. *Mol Microbiol* **28**, 281-291 (1998).
35 Sassanfar, M. & Roberts, J. Constitutive and UV-mediated activation of RecA protein: combined effects of recA441 and recF143 mutations and of addition of nucleosides and adenine. *J Bacteriol* **173**, 5869-5875 (1991).
36 Karu, A. E. & Belk, E. D. Induction of E. coli recA protein via recBC and alternate pathways: quantitation by enzyme-linked immunosorbent assay (ELISA). *Mol Gen Genet* **185**, 275-282 (1982).
37 Wang, X., Lesterlin, C., Reyes-Lamothe, R., Ball, G. & Sherratt, D. J. Replication and segregation of an Escherichia coli chromosome with two replication origins. *Proc Natl Acad Sci U S A* **108**, E243-250, doi:10.1073/pnas.1100874108 (2011).
38 Lesterlin, C., Pages, C., Dubarry, N., Dasgupta, S. & Cornet, F. Asymmetry of chromosome Replichores renders the DNA translocase activity of FtsK essential for cell division and cell shape maintenance in Escherichia coli. *PLoS Genet* **4**, e1000288, doi:10.1371/journal.pgen.1000288 (2008).
39 White, M. A., Eykelenboom, J. K., Lopez-Vernaza, M. A., Wilson, E. & Leach, D. R. Non-random segregation of sister chromosomes in Escherichia coli. *Nature* **455**, 1248-1250, doi:10.1038/nature07282 (2008).
40 Espeli, O., Mercier, R. & Boccard, F. DNA dynamics vary according to macrodomain topography in the E. coli chromosome. *Mol Microbiol* **68**, 1418-1427, doi:10.1111/j.1365-2958.2008.06239.x (2008).
41 McGinness, K. E., Baker, T. A. & Sauer, R. T. Engineering controllable protein degradation. *Mol Cell* **22**, 701-707, doi:10.1016/j.molcel.2006.04.027 (2006).
42 Reyes-Lamothe, R., Sherratt, D. J. & Leake, M. C. Stoichiometry and architecture of active DNA replication machinery in Escherichia coli. *Science* **328**, 498-501, doi:10.1126/science.1185757 (2010).
43 Helmstetter, C. E. *et al.* in *Escherichia coli and Salmonella* Vol. 2 (ed F. C. Neidhardt) 1627-1639 (ASM Press, 1996).
44 Kuwada, N. J., Cheveralls, K. C., Traxler, B. & Wiggins, P. A. Mapping the driving forces of chromosome structure and segregation in Escherichia coli. *Nucleic Acids Res*, doi:10.1093/nar/gkt468 (2013).

EXTENDED FIGURE LEGENDS

Extended Data Figure 1

(a) DSBs were introduced using the I-SceI endonuclease. The I-SceI cutting site (*I-SceI*^{CS}) is a 18 bp site (5'-TAGGGATAACAGGGTAAT-3') which was inserted 1067 kb from *oriC* on the Right replichore (*codA-cynR* intergenic region). *I-SceI*^{CS} is flanked by an upstream *parS-P1* site (USe; 1.2 kb upstream of the cut) and a downstream *parS-PMT1* site (DSe; 0.6 kb downstream of the cut) that binds different fluorescent ParB proteins. *In vivo* localisation of USe and DSe was monitored in live cells by expressing the fluorescent fusions of the corresponding ParBP1 and ParBPMT1 binding proteins from pFHC2973 or pMS11. *I-SceI* gene controlled by the arabinose-inducible promoter was expressed from the *araB* locus of the chromosome (782 kb from *oriC*), or alternatively expressed from a plasmid when higher level of cutting was required. Two alleles of the *I-SceI* gene were used, namely the *wt* allele and an unstable allele carrying a degron tag (*I-SceI*$_{MycDas}$). The construction of the system is detailed in the Supplemental Experimental Procedures.

(b) Cell viability of Rec^{+} and *recA* cells assayed by plating efficiency after induction of *I-SceI*$_{MycDas}$. Colony forming units (Cfu/ml) were counted 0, 30, 60, 120 and 180 min after addition of 0.2 % arabinose in a steady-state population (OD_{600}=0.2). Values at t=0 were normalized to 1. Below, Southern blot shows the efficiency of DSB induction for the same time points, and the level of DSB measured from three independent experiments. A *cynT* probe (500 bp) was used to visualize the substrate: a 12 kb *SacII* fragment containing the *I-SceI* cut site, or the product of restriction by I-SceI (downstream 3.1 kb fragment). Conditions were used in which 60 min after I-SceI was induced, most cells with segregated sisters received no more than a single DSB, consistent with the overall level of cutting observed biochemically (~57 %) and the dependence on RecA for survival.

(c) Flow cytometry showing the DNA content distribution of TB28 strains in stationary phase, exponential growth (M9 glucose 30ºC) and after rifampicin/cephalexin run-out. Sub-populations harbouring 1 or 2 chromosome equivalents after run-out indicate the number of replication origins per cell (1.91), which was used to calculate the C+D period (74 min) using Helmstetter's model (origin per cell=$2^{(C+D)/t}$)[43]. A summary of the cell cycle parameters is shown. All experiments were performed in identical growth conditions where cells harbor only one replicating chromosome, with initiation of replication occurring ~6 min after birth in the T=80 min cell cycle.

(d) Snapshot analysis of USe localisation before (left) and after (right) 60 min of DSB induction showed an identical pattern compared to DSe (Fig. 1a). From left to right: ratio of cells with 0, 1 or 2 foci, dotplots of USe foci position as a function of cell length, histograms of USe position along the cell long axis and the inter-sister distance (ISD in μm) are shown. Below, a plot of ISD against cell length shows that DSB-induction triggers the global decrease of ISD values and generates a population of long cells with reduced ISD (framed in green) revealing the pairing of sister loci.

Extended Data Figure 2

(a) Analysis of DSB-induced DSe sister pairing events in Rec^+ cells. (i) Time-lapse particle tracking of DSe foci (5 min/frame) with indicative images (every 20 min) show pairing between segregated sister loci (DSB was induced 30 minutes before the beginning of time-lapse acquisition). The red dashed line indicates the sister-pairing event and the grey area indicates the pairing period. (ii) DSe focus fluorescence intensity quantification performed on two consecutive frames, i.e., before and after pairing, shows that the 1-focus observed after pairing retained 104 ±15 % of the added fluorescence of the previous sister focus (normalized at 100%) consistent with colocalization of the two localization arrays. (iii) Distance between DSe and USe foci centers remained unchanged upon DSB-induction in Rec^+ and *recA* cells, indicating that both DNA ends remain coincident throughout cutting, pairing and repair. (iv) Summary diagram of sister pairing

that occurred 103 ±46 min after DSB-induction and lasted for 50 ±34 min (grey area). Once initiated, pairing occurred rapidly (<5 min) and engaged both DSB ends.

(b) DSB-induction generated a variety of cell-types harboring 0, 1 or 2 DSe foci with 0, 1 or 2 USe due to loss of the DSe or/and USe foci. One image for each of the 9 cell-types is shown with their quantification 0, 60 and 120 min after DSB-induction in Rec^+ and *recA* strains. These data are represented by a square density representation. This was obtained using custom MATLAB code that uses the data generated by the spotfinderM function of MicrobeTracker software. Only cells >3.3 μm are considered in order to focus the analysis on the fraction of cells in which the I-SceI cut site region (*codA-cynR*) has already segregated. (ii) Two-colour time-lapse analysis after DSB-induction showed that DSe and USe foci belonging to the same DSB disappeared within 0-5 min from one another in 71 % of cases (green and red lines), and recovered within 0-10 min from one another in 87 % of cases (green and red arrows) consistent with bidirectional processing of the two ends of the DSB by RecBCD (See Supplementary Discussion).

(c) Time-lapse analysis of RecBCD-mediated complete degradation of the nucleoid after DSB-induction in *recA* cells. One example is shown with nucleoid DNA stained with DAPI (green), cell membranes stained with FM4-64 (red). The decrease in fluorescence intensity of nucleoids undergoing degradation (red curve) was measured and reflects the rate of DNA degradation *in vivo* (Video S1). Decrease in fluorescence of non-degraded nucleoids is accounted for by photobleaching of the DAPI (blue curve). The overall rate of DNA degradation was 23.2 kb/min (386 bp/s) i.e., 193 bp/s/RecBCD complex (n=38 cells analysed).

Extended Data Figure 3

(a) Survival after UV-irradiation shows complementation of *recA-gfp* allele sensitivity (SS0385 strain) by expression of a wild-type *recA* gene in the *fhuB* ectopic locus of the chromosome or from a plasmid (pSC101-*recA*). RecA-GFP strain (TB28, *recA-gfp, fhuB::recA*) showed a level of UV-resistance similar to the *wt* strain.

(b) Snapshot analysis of RecA-GFP structures induced by DSBs. Each image was obtained by projection of a 3D stack (15 z-sections of 125 nm z-distance) of 3D-SIM images for RecA-GFP (green) merged with conventional images for DSe (red). Before DSB-induction, RecA is diffuse in most cells (95 %) and spontaneous spots are distant from DSe foci. 60 min after DSB-induction, RecA spots form in close proximity to a DSe focus and RecA bundles are observed in 29 % of total cells, regardless of whether cells have 1 or 2 DSe foci. In cells with 2 DSe and RecA bundle, 47 % of RecA-GFP bundles were associated with 1 DSe focus and 44 % were associated with both DSe foci. Bundle length, as well as the thickness of the large central body and the thinner extensions is shown in the histogram on the left (nm). The width of the thinner extensions (≤120 nm) corresponds to the lateral resolution limit of 3D-SIM. See Video S2-7.

(c) Fluorescence recovery after photobleaching (FRAP) of RecA bundles. Fluorescence intensities of bleached (green curve) and non-bleached regions (blue curve) of RecA bundles were monitored up to 1,500 sec after bleaching. No fluorescence recovery was observed throughout this period as shown by the indicative time-lapse images below. The green and the blue boxes indicate the bleached and non-bleached regions of the bundle (time in s). Initial fluorescence was normalized to 1 (Video S3).

(d) RecA bundle formation after UV-irradiation. The ratio of cells with RecA bundle(s) after irradiation with ultra violet light (50 J/M^2) was measured, as was the total fluorescence intensity of RecA-GFP. The level of the SOS response was reported by the expression of the *m-cherry* gene controlled by *PsulA* SOS-inducible promoter. Time-lapse of RecA-GFP after UV-irradiation confirms rapid bundle formation after UV treatment and snapshot images show multiple bundles present in most cells 45 min after UV-irradiation (Video S8).

(e) Relative frequencies of RecA bundles and RecA spots 60 min after DSB-induction at *codA* (356.6 kb) or *ydeO* (1581.7 kb) cut sites. *YdeO* and *codA* loci have different replication-segregation timings as manifested by the fractions of 2-focus cells (8 % and 69 %, respectively). Images below show the morphology of RecA bundles observed in those two cell populations (See Supplementary Discussion).

Extended Data Figure 4

(a) Mobility analysis of uncut loci (left) and both the long-traveling (blue) and the short-travelling (red) sister foci during DSB-induced sister pairing. From the MSDs, we calculated a MSD scaling parameter α=0.5 for the uncut locus compared to 0.69 for the long-travelling sister and 0.41 for the short-travelling one. This compares to α=1 for diffusive movement and α=2 for processive movement[44].

(b) Survival after UV-irradiation of cells expressing RecN-, PriA- and RecG-YPet fluorescent proteins expressed from their endogenous promoters in their normal chromosomal position. All four fusion proteins were recombination-proficient as demonstrated by resistance to UV irradiation.

(c) Histogram of the fraction of cells harbouring RecN-YPet, RecG-YPet or PriA-YPet fusions showing DSB-induced focus formation in Rec^+, but not in *recB* cells. Averages and standard deviations are calculated form snapshot images of three independent experiments. Below, the percentage of RecN-YPet, PriA-YPet and RecG-YPet spots that colocalised (<0.5 μm apart) with DSe focus is shown with indicative images. Residence times (s) of these foci, estimated by time-lapse analysis, are indicated (See Supplementary Discussion).

Extended Data Figure 5

(a) Immunocytochemistry using anti-RecA antibodies and Alexa-594-conjugated secondary antibodies. Left, bundles formed by wild-type RecA 60 min after DSB-induction (in >25 % of analyzable cells) or 10 min after UV-induction (in >80 % of analyzable cells). Right, in the RecAwt / RecA-GFP diploid strain; bundles were visualized both by immunocytochemistry and by direct observation of RecA-GFP.

(b) Visualization of RecA803-Rfp upon DNA damage induction. Merge of phase contrast and RFP images acquired with conventional fluorescent microscopy are shown. RecA803-RFP appeared diffuse in the cell before damage induction, and showed bundle formation similar to that observed with the RecA-GFP fusion after DSB-induction (same

conditions than in Fig. 1 and 2) or UV-irradiation (10 J/M^2). Histogram presents the fractions of cells with RecA803-RFP bundles in corresponding conditions.

(c) Survival of cells carrying different *recA* alleles after DSB induction and UV-irradiation (10 J/m^2), estimated by a plating assay.

(d) 3D-SIM images of RecA-GFP, RecAK72A-GFP and RecAK72R-GFP fusions after DSB-induction (same conditions than in Fig. 1 and 2) or UV-induction (10 J/M^2). Histograms present the fraction of cells with diffuse fluorescence, cells with RecA spots or RecA bundles ('others' corresponds to cells with saturated signal or aberrant morphologies).

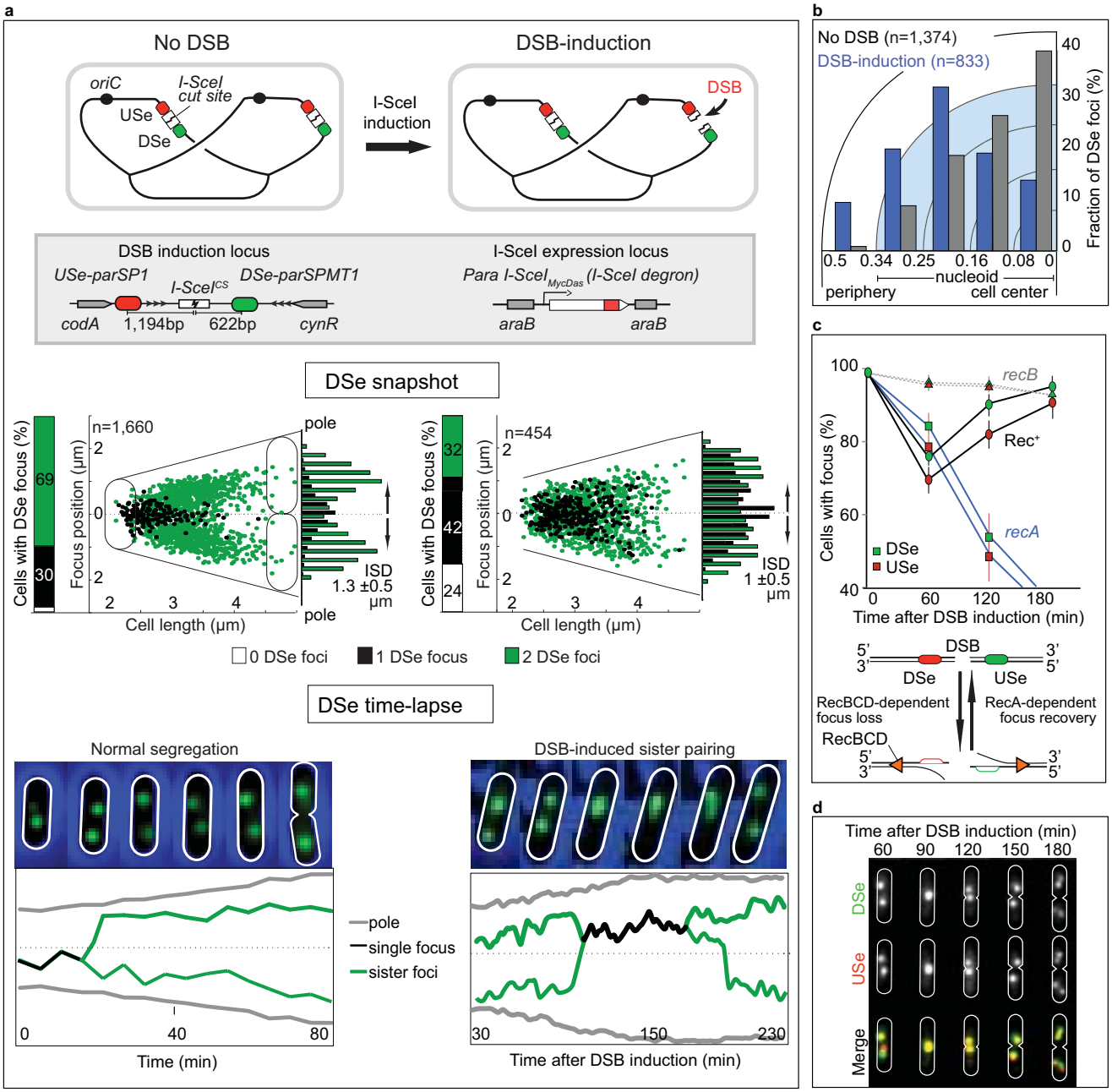
a
No DSB
DSB-induction
oriC
I-SceI cut site
USe
DSe
I-SceI induction
DSB
DSB induction locus
USe-parSP1
I-SceI^CS
DSe-parSPMT1
codA
1,194bp
622bp
cynR
I-SceI expression locus
Para I-SceI MycDas (I-SceI degron)
araB
araB
DSe snapshot
Cells with DSe focus (%)
69
30
n=1,660
Focus position (µm)
pole
ISD
1.3 ±0.5 µm
Cell length (µm)
32
42
24
n=454
ISD
1 ±0.5 µm
0 DSe foci
1 DSe focus
2 DSe foci
DSe time-lapse
Normal segregation
DSB-induced sister pairing
pole
single focus
sister foci
Time (min)
Time after DSB induction (min)
b
No DSB (n=1,374)
DSB-induction (n=833)
Fraction of DSe foci (%)
0.5 0.34 0.25 0.16 0.08 0
nucleoid
periphery
cell center
c
Cells with focus (%)
recB
Rec+
recA
DSe
USe
Time after DSB induction (min)
DSB
RecBCD-dependent focus loss
RecA-dependent focus recovery
RecBCD
d
Time after DSB induction (min)
DSe
USe
Merge

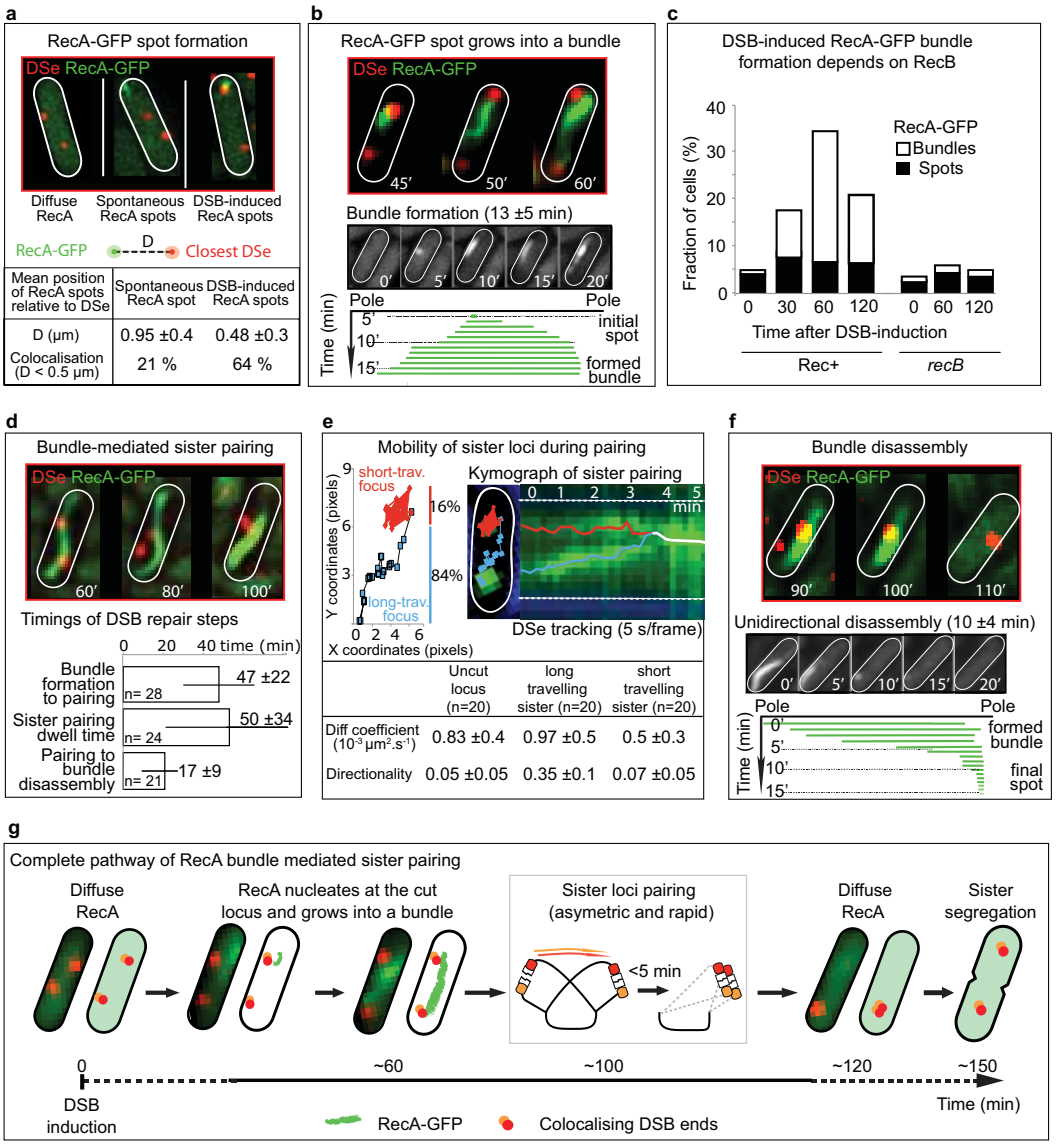
a
RecA-GFP spot formation
DSe RecA-GFP
Diffuse RecA
Spontaneous RecA spots
DSB-induced RecA spots
RecA-GFP
D
Closest DSe
Mean position of RecA spots relative to DSe
Spontaneous RecA spot
DSB-induced RecA spots
D (µm)
0.95 ±0.4
0.48 ±0.3
Colocalisation (D < 0.5 µm)
21 %
64 %
b
RecA-GFP spot grows into a bundle
DSe RecA-GFP
45′
50′
60′
Bundle formation (13 ±5 min)
0′
5′
10′
15′
20′
Pole
Pole
Time (min)
5′
10′
15′
initial spot
formed bundle
c
DSB-induced RecA-GFP bundle formation depends on RecB
Fraction of cells (%)
RecA-GFP
Bundles
Spots
Time after DSB-induction
Rec+
recB
d
Bundle-mediated sister pairing
DSe RecA-GFP
60′
80′
100′
Timings of DSB repair steps
time (min)
Bundle formation to pairing
n= 28
47 ±22
Sister pairing dwell time
n= 24
50 ±34
Pairing to bundle disassembly
n= 21
17 ±9
e
Mobility of sister loci during pairing
short-trav. focus
long-trav. focus
16%
84%
Y coordinates (pixels)
X coordinates (pixels)
Kymograph of sister pairing
min
DSe tracking (5 s/frame)
Uncut locus (n=20)
long travelling sister (n=20)
short travelling sister (n=20)
Diff coefficient (10⁻³ µm².s⁻¹)
0.83 ±0.4
0.97 ±0.5
0.5 ±0.3
Directionality
0.05 ±0.05
0.35 ±0.1
0.07 ±0.05
f
Bundle disassembly
DSe RecA-GFP
90′
100′
110′
Unidirectional disassembly (10 ±4 min)
0′
5′
10′
15′
20′
Pole
Pole
Time (min)
0′
5′
10′
15′
formed bundle
final spot
g
Complete pathway of RecA bundle mediated sister pairing
Diffuse RecA
RecA nucleates at the cut locus and grows into a bundle
Sister loci pairing (asymetric and rapid)
<5 min
Diffuse RecA
Sister segregation
0
~60
~100
~120
~150
DSB induction
Time (min)
RecA-GFP
Colocalising DSB ends

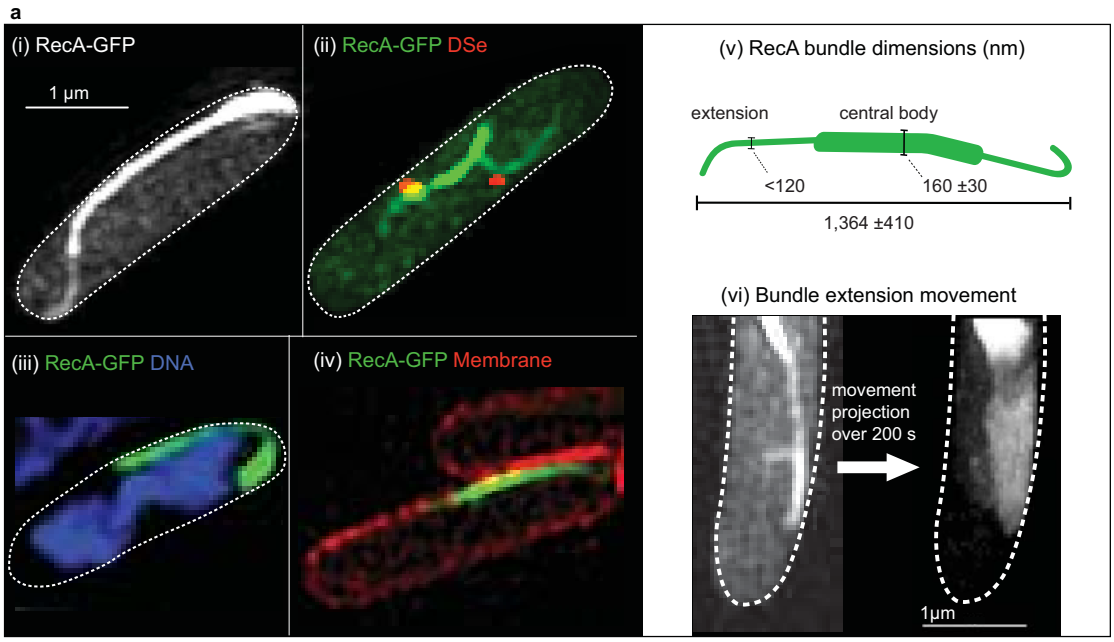
a
(i) RecA-GFP
1 µm
(ii) RecA-GFP DSe
(iii) RecA-GFP DNA
(iv) RecA-GFP Membrane
(v) RecA bundle dimensions (nm)
extension
central body
<120
160 ±30
1,364 ±410
(vi) Bundle extension movement
movement projection over 200 s
1µm

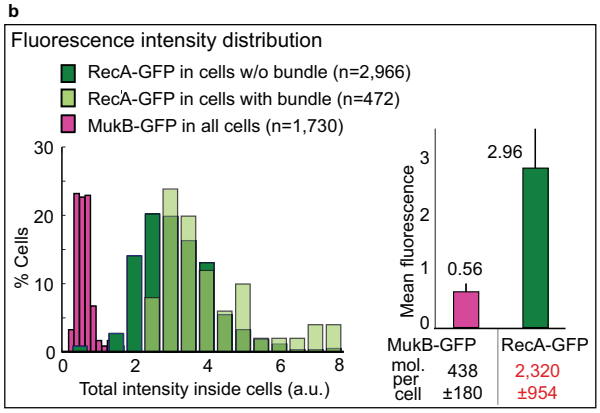
b
Fluorescence intensity distribution
RecA-GFP in cells w/o bundle (n=2,966)
RecA-GFP in cells with bundle (n=472)
MukB-GFP in all cells (n=1,730)
% Cells
Total intensity inside cells (a.u.)
Mean fluorescence
0.56
2.96
MukB-GFP
RecA-GFP
mol. per cell
438 ±180
2,320 ±954

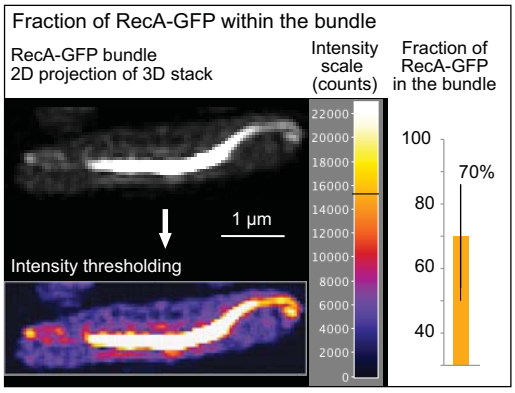
c
Fraction of RecA-GFP within the bundle
RecA-GFP bundle 2D projection of 3D stack
Intensity scale (counts)
Fraction of RecA-GFP in the bundle
1 µm
Intensity thresholding
70%

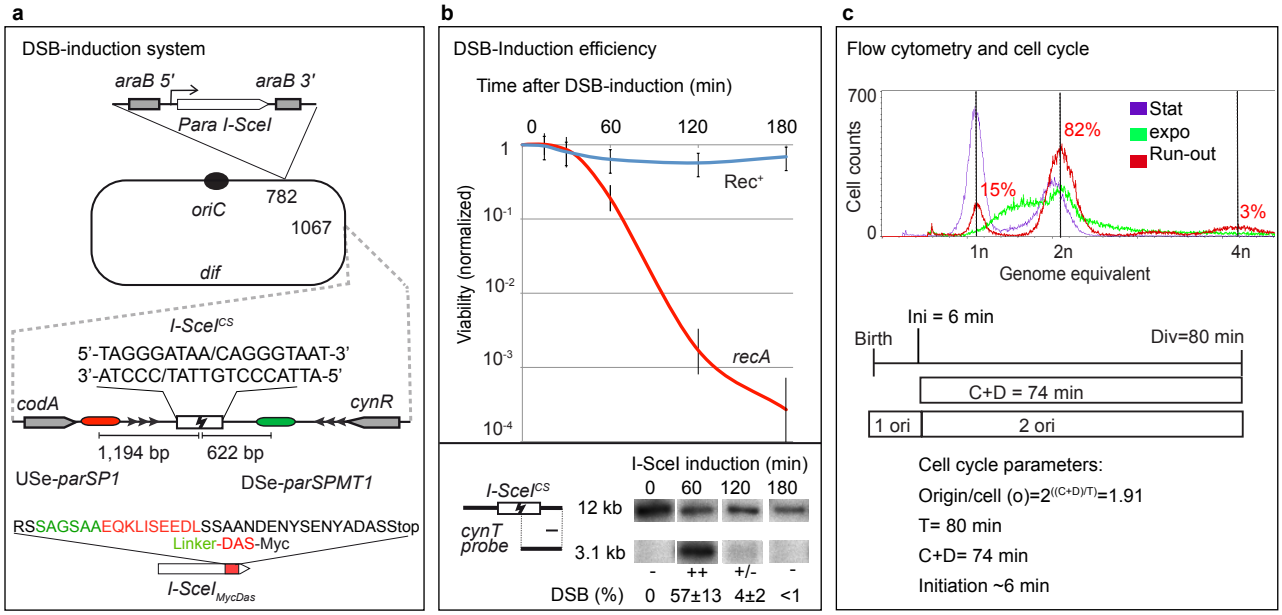
a
DSB-induction system
araB 5'
araB 3'
Para I-SceI
782
oriC
1067
dif
I-SceI^CS
5'-TAGGGATAA/CAGGGTAAT-3'
3'-ATCCC/TATTGTCCCATTA-5'
codA
cynR
1,194 bp
622 bp
USe-parSP1
DSe-parSPMT1
RSSAGSAAEQKLISEEDLSSAANDENYSENYADASStop
Linker-DAS-Myc
I-SceI MycDas
b
DSB-Induction efficiency
Time after DSB-induction (min)
0
60
120
180
1
10-1
10-2
10-3
10-4
Viability (normalized)
Rec+
recA
I-SceI induction (min)
0
60
120
180
I-SceI^CS
cynT probe
12 kb
3.1 kb
-
++
+/-
-
DSB (%)
0
57±13
4±2
<1
c
Flow cytometry and cell cycle
700
0
Cell counts
Stat
expo
Run-out
82%
15%
3%
1n
2n
4n
Genome equivalent
Ini = 6 min
Birth
Div=80 min
C+D = 74 min
1 ori
2 ori
Cell cycle parameters:
Origin/cell (o)=2((C+D)/T)=1.91
T= 80 min
C+D= 74 min
Initiation ~6 min

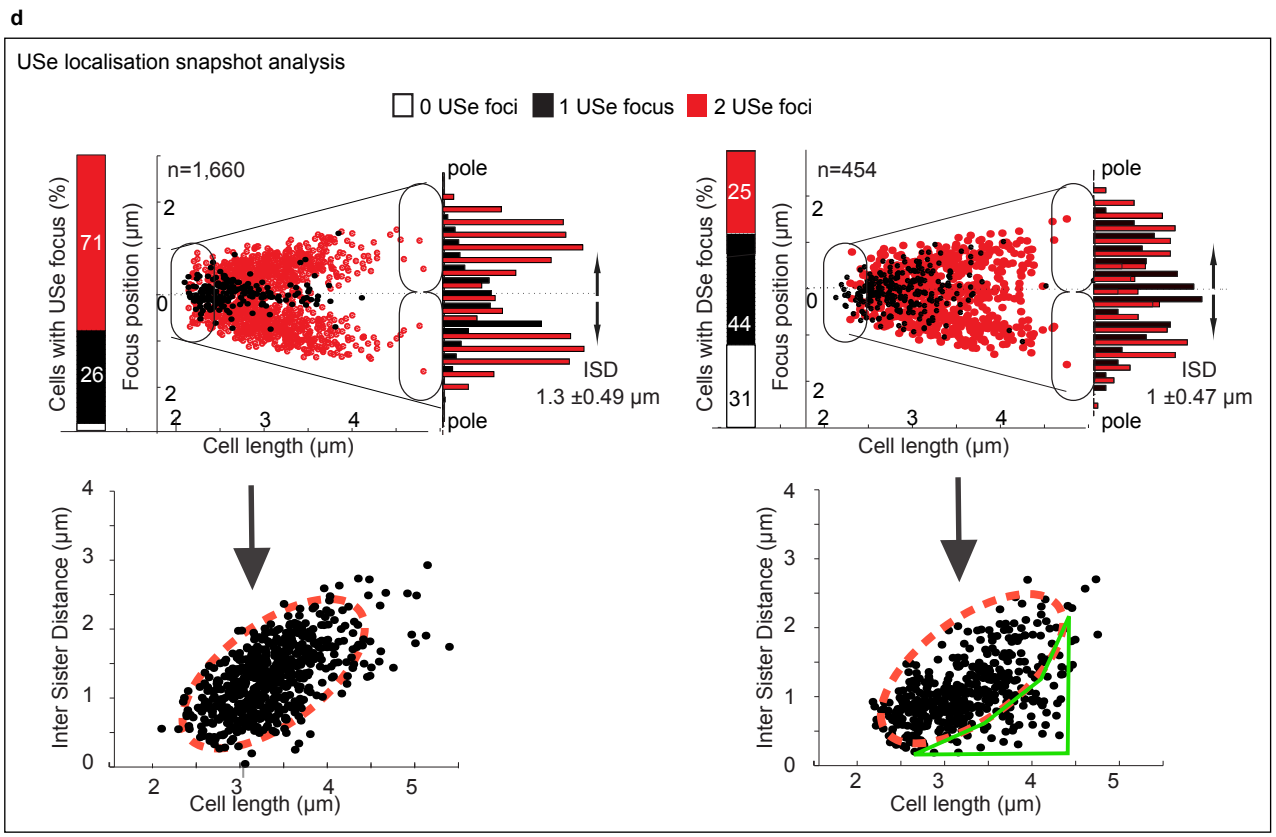
d
USe localisation snapshot analysis
0 USe foci
1 USe focus
2 USe foci
n=1,660
Cells with USe focus (%)
71
26
Focus position (µm)
pole
pole
ISD
1.3 ±0.49 µm
Cell length (µm)
n=454
Cells with DSe focus (%)
25
44
31
ISD
1 ±0.47 µm
Inter Sister Distance (µm)
Cell length (µm)

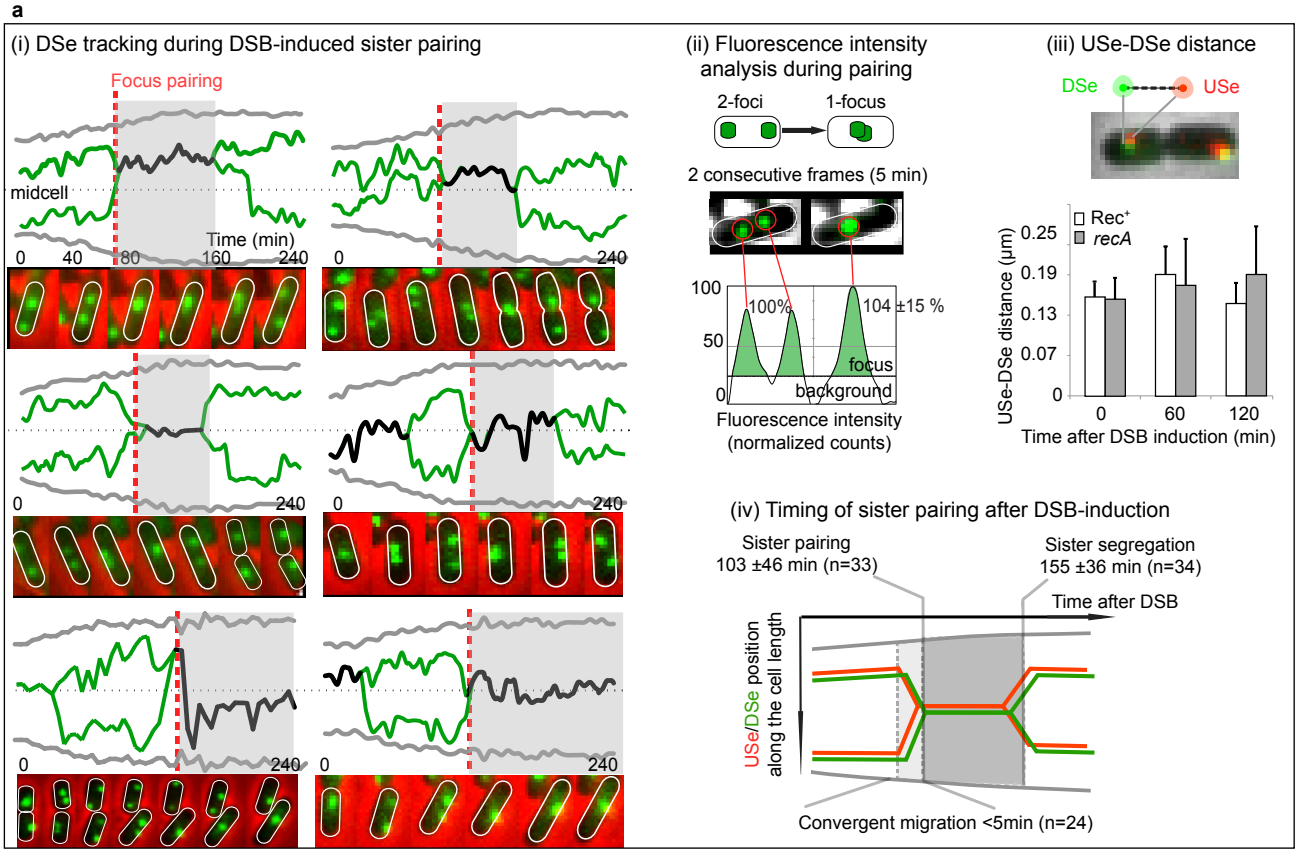
a
(i) DSe tracking during DSB-induced sister pairing
Focus pairing
midcell
Time (min)
0 40 80 160 240
(ii) Fluorescence intensity analysis during pairing
2-foci
1-focus
2 consecutive frames (5 min)
100%
104 ±15 %
focus
background
Fluorescence intensity (normalized counts)
(iii) USe-DSe distance
DSe
USe
Rec+
recA
USe-DSe distance (µm)
Time after DSB induction (min)
(iv) Timing of sister pairing after DSB-induction
Sister pairing 103 ±46 min (n=33)
Sister segregation 155 ±36 min (n=34)
Time after DSB
USe/DSe position along the cell length
Convergent migration <5min (n=24)

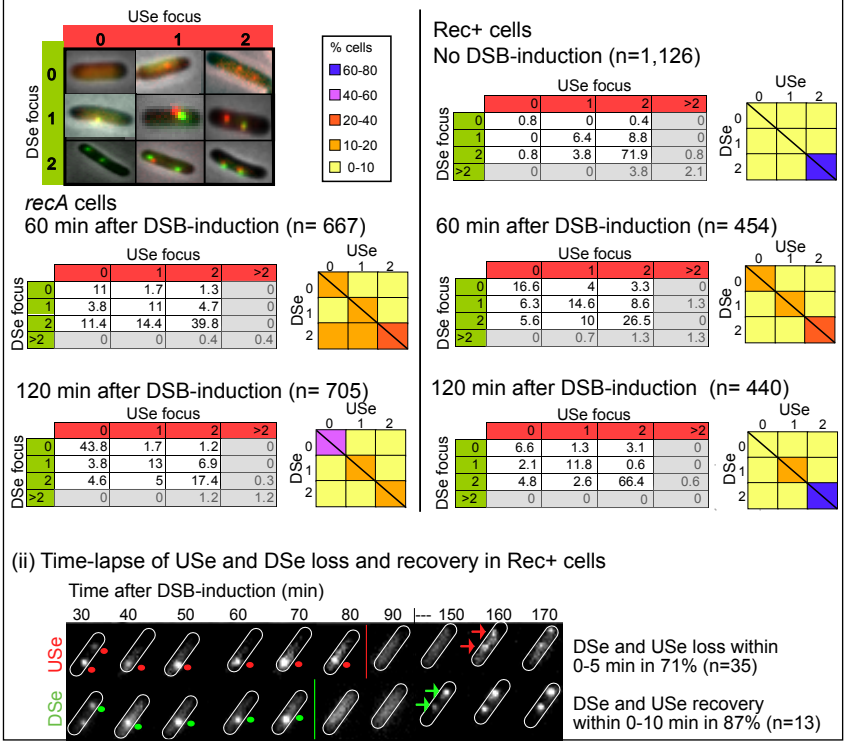
b
(i) Fraction of cell-types after DSB-induction in Rec+ and recA cells (%)
USe focus
DSe focus
% cells
60-80
40-60
20-40
10-20
0-10
recA cells
60 min after DSB-induction (n= 667)
120 min after DSB-induction (n= 705)
Rec+ cells
No DSB-induction (n=1,126)
60 min after DSB-induction (n= 454)
120 min after DSB-induction (n= 440)
(ii) Time-lapse of USe and DSe loss and recovery in Rec+ cells
Time after DSB-induction (min)
USe
DSe
DSe and USe loss within 0-5 min in 71% (n=35)
DSe and USe recovery within 0-10 min in 87% (n=13)

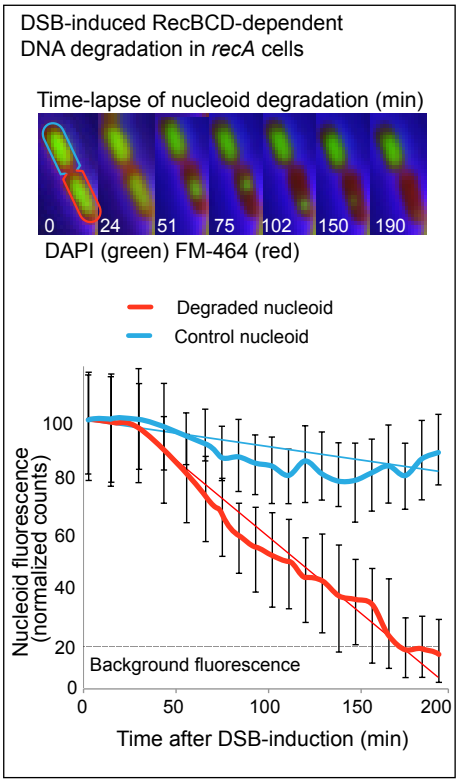
c
DSB-induced RecBCD-dependent DNA degradation in recA cells
Time-lapse of nucleoid degradation (min)
DAPI (green) FM-464 (red)
Degraded nucleoid
Control nucleoid
Nucleoid fluorescence (normalized counts)
Background fluorescence
Time after DSB-induction (min)

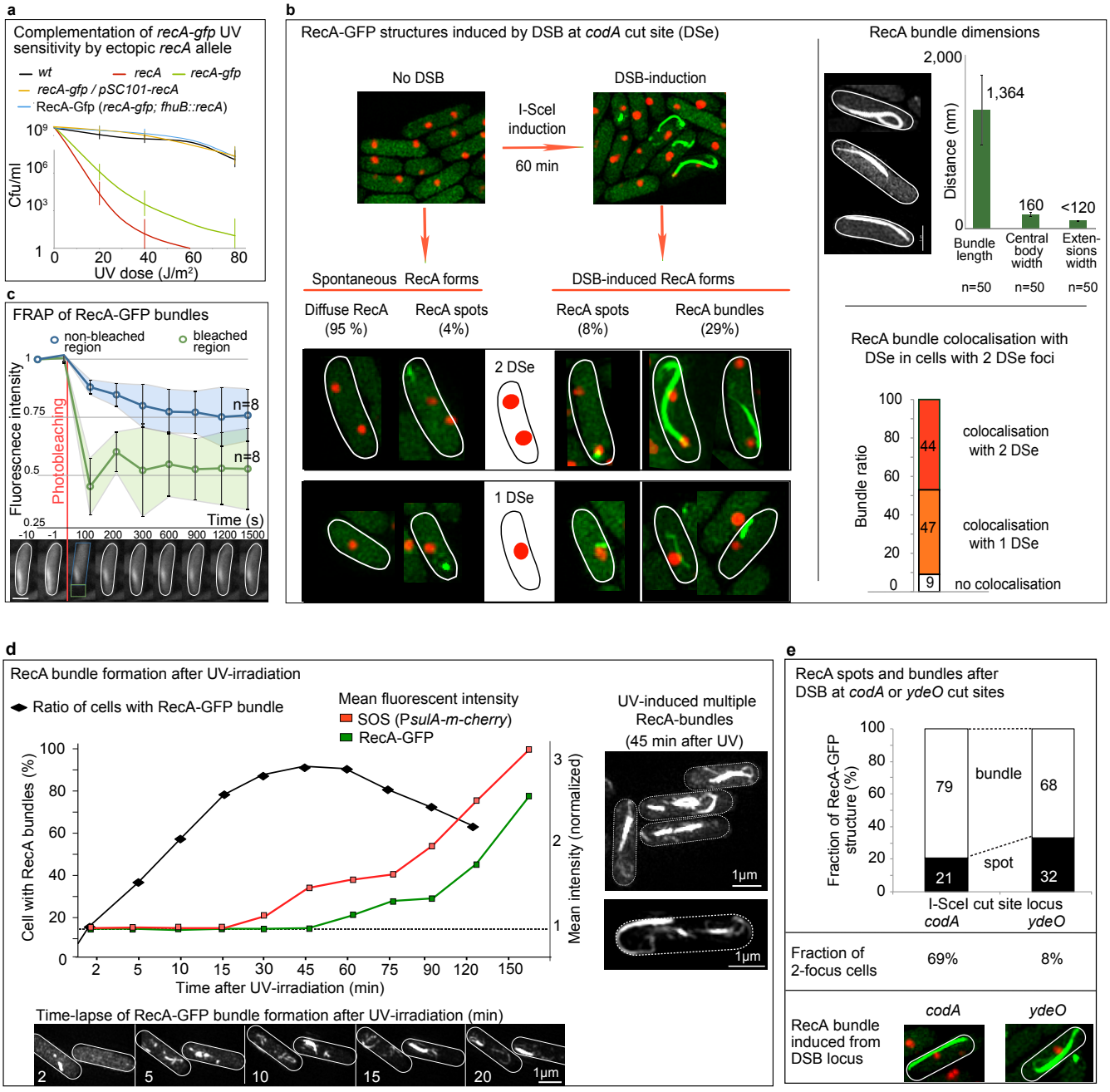

Extended Data Fig. 3

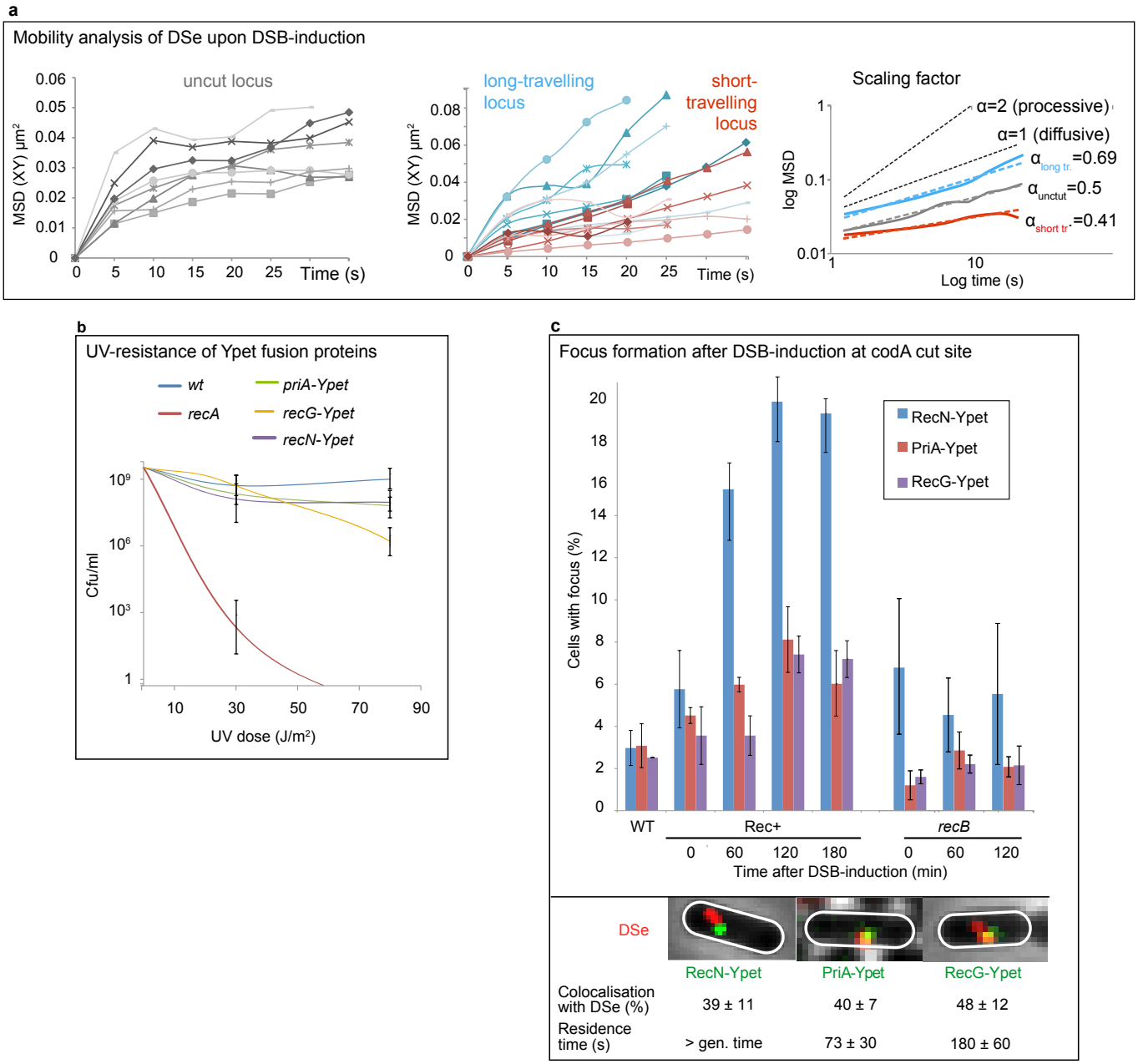

Extended Data Fig. 4

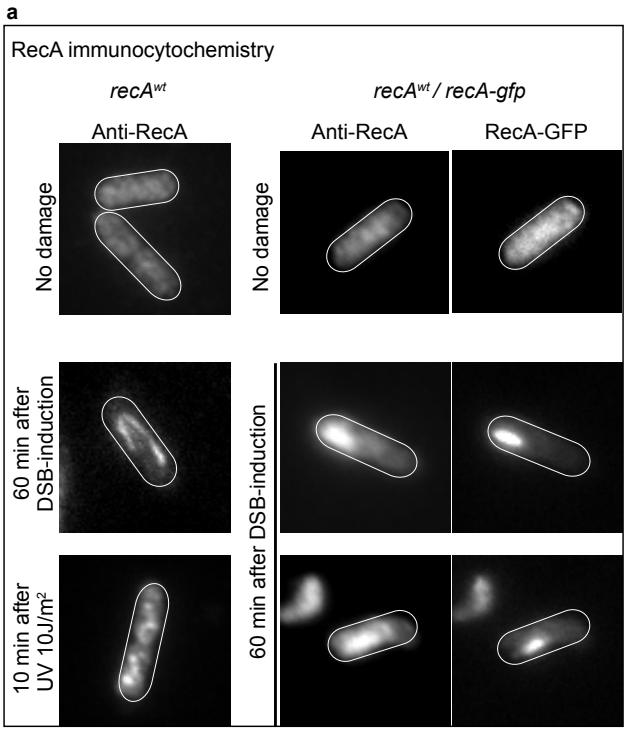

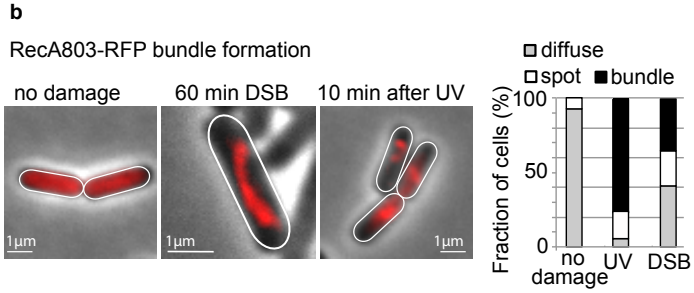

c

recA allele	Survival after UV-irradiation (10 J/m²) (%)	Survival after DSB-indution (%)	Distant sister pairing
*recA^wt^*	63 ±13	65 ±8	+++
recA-	< 0.001	< 0.1	-
recA-gfp	<1	25 ±12	n.d
recA-gfp; recAwt	35 ±12	62 ±5	+++
recAK72A-gfp	< 0.001	< 0.1	-
recAK72R-gfp	< 0.001	< 0.1	-
recA803-rfp	47 ±12	n.d	n.d

n.d: not determined

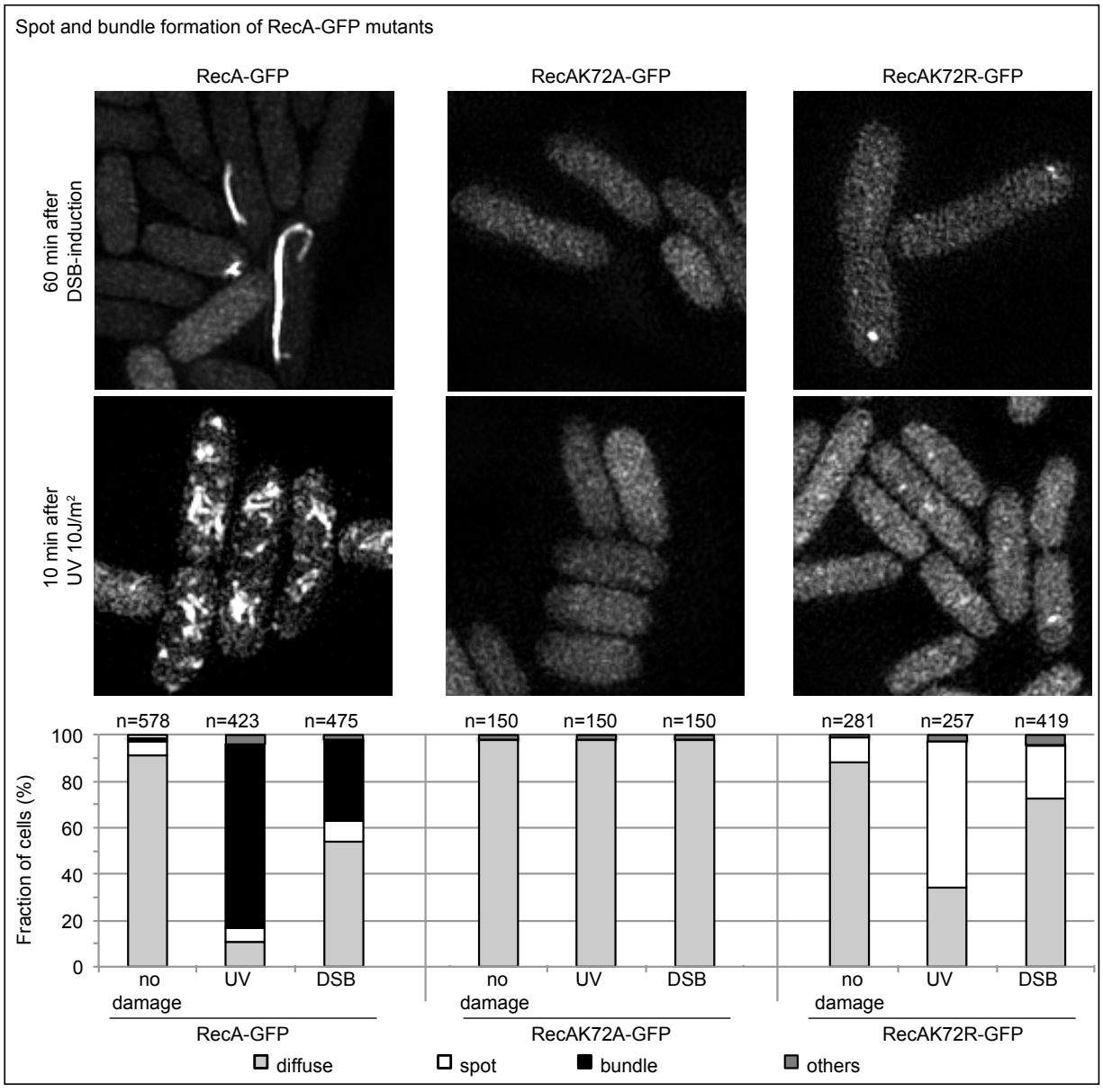

SUPPLEMENTARY INFORMATION

This file contains Supplementary Video legends, Supplementary Tables and Supplementary Discussion.

SUPPLEMENTARY VIDEO LEGENDS

Video S1 Time-lapse of nucleoid degradation after DSB-induction in *recA* cells. From the left: Merge, Phase-contrast, DAPI, FM4-64 (3 min/frame over 190 min). Cell-by-cell differences are due to the fact that induction of DSBs is asynchronous in the population.

Video S2 Time-lapse of RecA bundle assembly (left) and directional disassembly (right) with corresponding fluorescence density dynamic plot (30 s/frame over 30 min).

Video S3 Fluorescence Recovery After Photobleaching of RecA bundles. Three experiments are shown, from 10 min before bleaching to 25 min after bleaching.

Video S4 3D-SIM of DSB-induced RecA bundles.

Video S5 3D-SIM of RecA bundles with DSe segregated foci.

Video S6 Time-lapse 3D-SIM of RecA bundles (2s/Frame).

Video S7 4D rendering of time-lapse 3D-SIM of RecA bundles (2s/Frame), with orthogonal view showing the rapid movement of the bundle extension.

Video S8 3D-SIM of a single cell with UV-induced multiple RecA bundles.

Supplementary Table 1. *Escherichia coli* K-12 strains

Strain name	Relevant genotypes [a]	Source[b]
Background strain used in this work		
TB28	MG1655 Δ*lacIZYA*	[1]
General P1 donors and initial λ-red constructs		
codA^{CS}	TB28 *codA::I-SceI*^{CS}*-frt-cat*	λ-Red oligo (O3/O4) pOX5 in TB28
ydeO^{CS}	TB28 *ydeO::I-SceI*^{CS}*-frt-cat*	λ-Red oligo (O5/O6) pOX5 in TB28
I-SceI$_{MycDas}$	TB28 *araB::P*$_{ara}$ *I-SceI*$_{MycDas}$ *frt-kan*	λ-Red oligo (araBup/do) pOX6 in TB28
fhuB::recA	TB28 *fhuB::recA*$_{wt}$*-frt-cat*	λ-Red oligo (O7/O8) pOX15 in TB28
SS3085	*kan-recA4155-gfp (4155,4136 [c]) referred as RecA-GFP*	[2]
VS90	*recAT233C-tn10*	[3]
recA803-rfp	TB28 *fhuB:: recA803-rfp-cat*	λ-Red oligo (O7/O8) pOX17 in TB28, insertion of *recA803-Rfp* at *fhuB* locus
recAK72A	TB28 *fhuB:: recAK72A-cat*	λ-Red oligo (O7/O8) pOX18 in TB28, insertion of *recAK72A* at *fhuB* locus
recAK72R	TB28 *fhuB:: recAK72R-cat*	λ-Red oligo (O7/O8) pOX19 in TB28, insertion of *recA72R* at *fhuB* locus
recAK72A-gfp	TB28 *fhuB:: recAK72A-gfp-cat*	λ-Red oligo (O7/O8) pOX21 in TB28, insertion of *recAK72A-gfp* at *fhuB* locus
recAK72R-gfp	TB28 *fhuB:: recAK72A-gfp-cat*	λ-Red oligo (O7/O8) pOX22 in TB28, insertion of *recA72R-gfp* at *fhuB* locus in TB28
JW2788	*recB(Del)::kan*	CGSC [c], [4]
priA-Ypet	TB28 *priA-Ypet frt-kan*	λ-Red oligo (*priA-YPetup/do*) for endogenous YPet fusion into TB28
precN-Ypet	TB28 *recN-Ypet frt-kan*	λ-Red oligo (*recN-YPetup/do*) for endogenous YPet fusion into TB28
recG-Ypet	TB28 *recG-Ypet frt-kan*	λ-Red oligo (*recG-YPetup/do*) for endogenous YPet fusion into TB28
MG1655 (TB28) and derivatives[d]		
TB28	MG1655 Δ*lacIZYA*	[1]
Ox269	*araB::P*$_{ara}$ *I-SceI*$_{MycDas}$ *frt-kan*	TB28 x P1. *I*-SceI$_{MycDas}$ to Km
Ox142	*codA::I-SceI*^{CS}*-frt-cat*	TB28 x P1.codA^{CS} to Cm
Ox144	*ydeO::I-SceI*^{CS}*-frt-cat*	TB28 x P1.ydeO^{CS} to Cm

recAwt/recA-gfp	*kan-recA4155-gfp fhuB::recA$_{wt}$-cat*	*fhuB::recA* x P1.SS3085 to Cm
Rec$^+$	*codA::I-SceI^{CS}-frt-cat araB::P$_{ara}$ I-SceI$_{MycDas}$ frt-kan*	ox142 x P1.*I*-SceI$_{mycDas}$ to Km
recA	*codA::I-SceI^{CS}-frt-cat araB::P$_{ara}$ I-SceI$_{MycDas}$-frt-kan recAT233C-Tn10*	Rec$^+$ x P1.VS90 to Tc
recB	*codA::I-SceI^{CS}-frt-cat araB::P$_{ara}$ I-SceI$_{MycDas}$ -frt-kan recB::tn10*	Rec$^+$ x P1.JW2788 to Km
RecA-GFP	Rec$^+$ *kan-recA4155-gfp*	Rec$^+$ x P1.SS3085 to Km
RecAwt/GFP	*codA::I-SceI^{CS}-frt-cat araB::P$_{ara}$ I-SceI$_{MycDas}$ kan-recA4155-gfp fhuB::recA-cat*	RecA-GFP x P1.*fhuB::recA* to Cm
RecA803-RFP	*codA::I-SceI^{CS}-frt araB::P$_{ara}$ I-SceI$_{MycDas}$ frt-kan fhub::recA803-rfp cat recAT233C-tn10*	Rec$^+$ x P1. *recA803-Rfp to Cm*
RecAK72A-GFP	*codA::I-SceI^{CS}-frt araB::P$_{ara}$ I-SceI$_{MycDas}$ frt-kan FhuB::recAK72A-gfp-cat recAT233C-tn10*	Rec$^+$ x *recAK72A-gfp* to Cm and P1.VS90 to Tc
RecAK72R-GFP	*codA::I-SceI^{CS}-frt araB::P$_{ara}$ I-SceI$_{MycDas}$ frt-kan fhuB::recAK72R-gfp-cat recAT233C-tn10*	Rec$^+$ x *recAK72R-gfp* to Cm and P1.VS90 to Tc
RecA-GFP *recB*	RecA-Gfp *recB(Del)::kan*	RecA-GFP x P1. *recA803-rfp to Cm*
ydeO^{CS} RecA-GFP	*ydeO::I-SceI^{CS}-frt-cat araB::P$_{ara}$I-SceI$_{MycDas}$-frt kan-recA-gfp*	RecA wt/GFP x P1.ydeO^{CS} to Cm
RecN-Ypet	Rec$^{+;}$ *recN-Ypet-kan*	Rec$^+$ x P1.wt priA-Ypet to Km
RecG-Ypet	Rec$^+$ *recG-Ypet-kan*	Rec$^+$ x P1.wt priA-Ypet to Km
PriA-Ypet	Rec$^+$ *priA-Ypet-kan*	Rec$^+$ x P1.wt priA-Ypet to Km
RecN-Ypet *recB*	*recB recN-Ypet-kan*	RecN-Ypet x P1. P1. JW2788 to Km
RecG-Ypet r*ecB*	*recB recG-Ypet-kan*	RecG-Ypet x P1. P1. JW2788 to Km
PriA-Ypet *recB*	*recB priA-Ypet-kan*	PriA-Ypet x P1. P1. JW2788 t Km

[a] *codA::I-SceI^{CS}* and *ydeO::I-SceI^{CS}* correspond to insertion of the I-SceI^{CS} cassette described above, into the *codA-cynR* (356.6 kb) or *ydeO-ydeP* (1581.7 kb) intergenic regions. *fhuB::recA* refers to the insertion of *recA* wild-type gene in the *fhuB* ectopic locus (171 kb). The abbreviations *kan, cat* refer to insertions conferring resistance to kanamycin (Km^r), chloramphenicol (Cm^r) respectively. Tn*10* confers resistance to tetracycline (Tc^r). MycDas stands for the Myc tag, 2-aa linker and the DAS+4 degron tag described above.

[b] Constructs were made using λ-Red recombination and were transferred by P1 transduction following standard procedures. The λ-Red constructs, oligonucleotides, template plasmid, and acceptor strain that have been used are indicated in the 'source' column.

[c] CGSC stands for the coli Genetic Stock Center

[d] Only the relevant additional genotype of the derivatives is shown.

Supplementary Table 2. *Plasmids*

Name	Construct and Usage	Source
pDL2655	Arabinose inducible expression of I-SceI endonuclease (CmR)	5
pOX6	Arabinose inducible exprssion of I-SceIMycDas (CmR, KmR)	Insertion of $_{MycDas\text{-}frt}$-*kan* in Cterm of I-SceI on pDL2655
pOX5	*Carries I-SceICS cassette (frt-cam-parSP1-frt-3χ^{+}-I-SceI^{CS}-parSPMT1-3χ^{-}) and used for λ-RED insertion to the chromosome* (CmR)	See Supplementary Experimental Procedures
pOX15	*Carries P_{recA} $RecA_{wt}$ and used for λ-RED insertion of the ectopic recA gene copy in the fhuB locus of the chromosome* (CmR, AmpR)	Insertion of P_{recA} RecA and frt-Cm in pUC19 MCS
pFH2709	*parBPMT1-CFP; parBP1-Ypet for simultaneous in vivo* localisation of *parSP1* and *parSPMT1* (AmpR)	6
pOX17	*Carries P_{recA} recA803-rfp and used for λ-RED insertion of the ectopic recA gene copy in the fhuB locus of the chromosome* (CmR, AmpR). recA803-rfp derived from pNG1[7]	Insertion of P_{recA} *recA803-rfp frt-cat* in pUC19 MCS
pOX21-23	*Carries P_{recA} recAK72A-gfp (21) and P_{recA} recAK72R-gfp (22) used for λ-RED insertion of the ectopic recA gene copy in the fhuB locus of the chromosome* (CmR, AmpR)	Insertion of P_{recA} *recA-gfp mutant frt-cat* in pUC19 MCS
pMS11	pSC101 *parBPMT1-Mcherry* *In vivo* localisation of *parSPMT1*	8
pKD3-*parSPMT1*	*parSPMT1* site associated with *frt-cat*	9
pKD3-*parSP1*	*parSP1* site associated with *frt-cat*	9
pKD46	Plasmid for λ-Red recombination	10
pCP20	Flp expression plasmid (resistance removal)	10
pROD60	Plasmid carrying the degron tag	11
pROD61	Plasmid carrying the gene encoding the Ypet	11
pSulA-Mcherry	Reporter plasmid for SOS induction	This work

Supplementary Table 3. *Oligonucleotides*

OLIGO	Sequence (5' to 3')	Description
O1	CCCCCCGGGCTGGTGGTCGATGCTGAGCTGGTGGACAC GCGCTGGCTGGTGGTACTAGTCTCGAGTAGGGATAACA GGGTAATGC	O1 and O2 were hybridised and amplified by PCR to obtain a 149bp dsDNA carrying Not1 and Swa1 sites in which *parSs* were inserted
O2	GGAGTACTGCTGGTGGGCGCAGACTCGCTGGTGGTCAC ATGGCGGCTGGTGGAGATCTGCGGCCGCATTACCCTGT TATCCCTA	
O3	CGACTGGGTTACAGCGAGCTTAGTTTATGCCGGATGCG CAGGAAACAGCTATGACCA	λ-Red insertion of *I-Sce1*^{CS} cassette in *codA-cynR* region
O4	GTTCAGTGCTCTACGTAGGCCGGATAAGGCGTTCACGC GTAAAACGACGGCCAGTG	
O5	TATTTGCTAACGAGTAGTCAACCACACACGCTGCGTAA GTAAAACGACGGCCAGTG	λ-Red insertion of *i-sce1*^{cs} cassette in *ydeO-ydeP* region
O6	AACAACGCGGGGCAGGGAATGGCTGCCCCATTTAATTC CAGGAAACAGCTATGACCA	
araBup	CCACATTGATTATTTGCACGGC	λ-Red insertion of *I-SceI* in *araB*
araBdo	AAGCACTCCATGATTGCGCG	
O7	TTCCATATAACGGCCCTGTACGCCTGGACGGATAAAGG TCTGCTATGTGGTGCTATCT	λ-Red C-terminal fusion of *recN* to *YPet*
O8	CGCCAGCGTCGCATCGGGCATCCGTTGTCGCGTAAACG CGATTGTGTAGGCTGGAGCTGC	λ-red insertion of *recA* in *fhuB* region
SceIMycDASdo	ACCCCTTTCAGGCGTTGGTTAGCGTTCGGTGTGCGGCCG CCATATGAATATCCTCCTTAG	C-terminal fusion of *I-SceI* gene with *Myc tag* DAS+4-degron
SceIMycDASup	CAAACTGCCGAACACTATCTCCTCCGAAACTTTCCTGA AAAGCTCGGCTGGCTCCGCTG	
recAXmaIup	CCCCCCGGGTGCAGACCTTGTGGCAACAATT	Insertion of P_{recA} *recA* into pUC19 MCS
recASacIdo	CCCGAGCTCGCAGATGCGACCCTTGTGTAT	
parS-P1 up	CCGCTCTTCATTTAAATAAGGAGGATATTCATATGGAC	Amplification of *parSP1* (*Swa1*) from pGBKD3-parSP1
parS-P1 do	CCGCTCTTCATTTAAATGGTCTGCTATGTGGTGCTATC	
parS-PMT1up	CCGCGGCCGCGAATTCAAGGAGGATATTCATATGGAC	Amplification of *parSPMT1*(*Not1)* from pGBKD3-parSPMT1
parS-PMT1do	CCGCGGCCGCGAATTCGGTCTGCTATGTGGTGCTATC	
recN-YPetup	CGTAATACACTGGCGAATGCGAAAGAACTGCTTGCAGC GAGCTCGGCTGGCTCCGCT	λ-Red C-terminal fusion of *recN* to *YPet*
recN-YPetdo	CGTTTTGCTGTTTACTCTGACCGTGAAGCAGGAAAAAA GTCATATGAATATCCTCCTTA	
recG-YPetup	AGAACGCTGGATGCCGGAGACGGAACGTTACTCGAATG CGAGCTCGGCTGGCTCCGCT	λ-Red C-terminal fusion of *recG* to *YPet*
recG YPetdo	GTAGGGTAACCTGAAATGGCGGTCTTCTCACTGCCGCC TTCATATGAATATCCTCCTTA	
priA-YPetup	GTGAAATGGGTGCTGGATGTTGATCCGATTGAGGGTGC GAGCTCGGCTGGCTCCGCT	λ-Red C-terminal fusion of *priA* to *YPet*
priA YPetdo	AATATTGAATTTTTCGATCCGCCTCGCATCGTGAGCGGT TCATATGAATATCCTCCTTA	

SUPPLEMENTARY DISCUSSION

Processing of DSB ends by RecBCD is bidirectional

We analyzed snapshots of cells after cutting was induced and measured the relative frequencies of sub-populations of cells in which DSe, USe, or both markers, had disappeared (Extended Data Fig. 2b). In Rec^+ cells, the reduction of cells with DSe and USe foci through degradation after 60 min of DSB-induction was followed by an almost complete recovery by 180 min. Reduction in focus number did not occur in *recB* cells, demonstrating that nucleolytic and/or helicase processing by RecBCD of *parS* sites in the vicinity of the DSB underlies focus reduction. The recovery of focus number after 60 min was dependent on functional RecA, thereby reporting the HR-dependent restoration of *parS* site integrity during the 180 min assay period. Time-lapse experiments enabled us to estimate a period of 143 ± 66 min between the loss and recovery of DSe foci, reflecting the time required for completion of DSB repair by HR.

The fate of the USe and the DSe associated with the same DSB was monitored at the single cell level using time-lapse analysis; disappearance of DSe and USe associated with the same of DSB locus occurred within 0-5 min in most cells (Extended Data Fig. 2b). Likewise recovery of DSe and USe occurred within 0-10min. These results support the view that processing of DSB ends by RecBCD is bidirectional from the locus of the cutting, consistent with loading of RecBCD complexes onto each end of the break. Furthermore, concomitant RecA-dependent recovery of associated DSe and USe foci strongly indicates that both DSB ends are engaged in the strand invasion of the homologous sequence and subsequent HR repair. Our estimate of the rate of *in vivo* DNA degradation by RecBCD in the absence of RecA was ~190 bp/s per RecBCD complex (Fig. 1c, d and Extended Data Fig. 2b, c; Video S1; Supplementary discussion). This is less than *in vitro* measurements reporting that RecBCD unwinds naked DNA at 336 bp/s after Chi-site recognition[12] and translocates at 549 bp/s[13]. This difference likely arises because the overall degradation rate by RecBCD *in vivo* reflects encounters with proteins bound to DNA, encounters with Chi sites, chromosome higher order structure, and RecBCD dissociation-association events.

Recruitment of recombination proteins after DSB-induction

Homology-directed strand invasion results in the formation of a D-loop that is thought to facilitate the recruitment of proteins required to complete repair by HR. PriA is

required for the restart of replication induced during recombinational repair[14], RecN and RecG are thought to be involved in the early and late stages of DSB repair, respectively[15-17]. We studied the localisation and timing of focus formation of these proteins fused to the YPet fluorescent protein and expressed from their endogenous promoters in their normal chromosomal position. All three fusion proteins were functional as demonstrated by resistance to ultraviolet light irradiation (Extended Data Fig. 4b). Before DSB induction, 2-6% of Rec^+ cells had fluorescent spots of PriA, RecN and RecG (Extended Data Fig. 4c), similar values to those observed in wild-type cells lacking the I-SceI cutting system. This presumably reflects both the frequency of endogenous repair events that use these proteins and the lifetimes of the individual protein complexes. These values are similar to the fraction cells that have fluorescent RecA spots or bundles before DSB-induction (Fig. 2c). The frequency of cells with a RecN focus reached a maximum ~60 min after DSB induction, as for RecA, whereas the PriA maximum was at ~120 min and the RecG maximum was between 120 and 180 min. About half of these spots were associated with DSe as shown by the fraction of colocalisation. RecN-, PriA- and RecG-focus increase was dependent on RecBCD, consistent with DSB processing being a prerequisite for recruitment of these proteins, as for RecA. The frequency of PriA and RecG foci was much lower than the level of DSBs, accounting for their limited residence time of ~73 s and ~180 s, respectively, measured by time-lapse analysis. RecN foci had a longer lifespan, suggesting that RecN is only recruited to a fraction of DSBs. These results show that DSB-induction is followed by recruitment of recombination factors that promote replication restart and recombination intermediate processing.

Stoichiometry and architecture of RecA bundles

The evidence that RecA bundles form from the normal RecA pool comes from the observation that ~80 % of cells had RecA bundles 15 min after UV-irradiation, before any SOS response and consequent RecA over-expression were detected (Extended Data Fig. 3d). UV-irradiated cells often contained several morphologically heterogeneous bundles, consistent with them being nucleated from multiple damaged loci (Video S8).

Because a RecA monomer binds to 3 nt within a RecA-ssDNA filament[25,26], the ~3200 RecA molecules in a bundle could potentially bind ~10^4 nt of ssDNA. However, the analyzed cells with bundles retained fluorescent ParB protein bound to its cognate dsDNA site, only ~600 bp from the DSB. Bidirectional processing of the

break by RecBCD should therefore lead to <1200 nt of ssDNA, bound by <400 RecA molecules, at the processed break. These ssDNA-RecA filaments would extend linearly for much less than the <630 nm maximum, because fluorescent ParB proteins bound to either side of a cut locus form overlapping spots (Fig. 1d). We conclude therefore that >85 % of RecA molecules present in bundles are likely to be DNA-free and additional to the two presynaptic ssDNA-RecA filaments that we propose nucleate bundle formation. The RecA filaments that can assemble *in vitro* into bundles by lateral interaction, were shorter than those characterized here[26-31].

RecA bundles form at similar frequencies regardless of whether sister homology is present

To address whether the formation of RecA bundles depends on the presence of a distant homologous sequence in the cell, we compared the frequency of bundle formation when the DSB was induced at the *codA* locus (356.6 kb), which was present as segregated sisters in 69% of cells, with that obtained when the DSB was introduced at the *dif* proximal *ydeO* locus (1581.7 kb), which is replicated last and present as segregated sisters in 8% of cells (Extended Data Fig. 3e). The results showed that the frequency of bundle formation after DSB induction is similar for both cut sites and is therefore insensitive to the state of replication-segregation of the damaged locus. In addition, no significant differences in bundle morphology were observed. This demonstrates that the formation of the bundle is blind to the presence of sister homology.

SUPPLEMENTARY REFERENCES

1 Bernhardt, T. G. & de Boer, P. A. Screening for synthetic lethal mutants in Escherichia coli and identification of EnvC (YibP) as a periplasmic septal ring factor with murein hydrolase activity. *Mol Microbiol* **52**, 1255-1269, doi:10.1111/j.1365-2958.2004.04063.x (2004).

2 Renzette, N. *et al.* Localization of RecA in Escherichia coli K-12 using RecA-GFP. *Mol Microbiol* **57**, 1074-1085, doi:10.1111/j.1365-2958.2005.04755.x (2005).

3 Sivanathan, V. *et al.* KOPS-guided DNA translocation by FtsK safeguards Escherichia coli chromosome segregation. *Mol Microbiol* **71**, 1031-1042, doi:10.1111/j.1365-2958.2008.06586.x (2009).

4 Baba, T. *et al.* Construction of Escherichia coli K-12 in-frame, single-gene knockout mutants: the Keio collection. *Molecular systems biology* **2**, 2006 0008, doi:10.1038/msb4100050 (2006).

5 White, M. A., Eykelenboom, J. K., Lopez-Vernaza, M. A., Wilson, E. & Leach, D. R. Non-random segregation of sister chromosomes in Escherichia coli. *Nature* **455**, 1248-1250, doi:10.1038/nature07282 (2008).

6 Nielsen, H. J., Ottesen, J. R., Youngren, B., Austin, S. J. & Hansen, F. G. The Escherichia coli chromosome is organized with the left and right chromosome arms in separate cell halves. *Mol Microbiol* **62**, 331-338, doi:10.1111/j.1365-2958.2006.05346.x (2006).

7 Rehrauer, W. M. & Kowalczykowski, S. C. Alteration of the nucleoside triphosphate (NTP) catalytic domain within Escherichia coli recA protein attenuates NTP hydrolysis but not joint molecule formation. *J Biol Chem* **268**, 1292-1297 (1993).

8 Stouf, M., Meile, J. C. & Cornet, F. FtsK actively segregates sister chromosomes in Escherichia coli. *Proc Natl Acad Sci U S A*, doi:10.1073/pnas.1304080110 (2013).

9 Espeli, O., Mercier, R. & Boccard, F. DNA dynamics vary according to macrodomain topography in the E. coli chromosome. *Mol Microbiol* **68**, 1418-1427, doi:10.1111/j.1365-2958.2008.06239.x (2008).

10 Datsenko, K. A. & Wanner, B. L. One-step inactivation of chromosomal genes in Escherichia coli K-12 using PCR products. *Proc Natl Acad Sci U S A* **97**, 6640-6645 (2000).

11 Reyes-Lamothe, R., Sherratt, D. J. & Leake, M. C. Stoichiometry and architecture of active DNA replication machinery in Escherichia coli. *Science* **328**, 498-501, doi:10.1126/science.1185757 (2010).

12 Spies, M., Amitani, I., Baskin, R. J. & Kowalczykowski, S. C. RecBCD enzyme switches lead motor subunits in response to chi recognition. *Cell* **131**, 694-705, doi:10.1016/j.cell.2007.09.023 (2007).

13 Finkelstein, I. J., Visnapuu, M. L. & Greene, E. C. Single-molecule imaging reveals mechanisms of protein disruption by a DNA translocase. *Nature* **468**, 983-987, doi:10.1038/nature09561 (2010).

14 Marians, K. J. PriA-directed replication fork restart in Escherichia coli. *Trends Biochem Sci* **25**, 185-189 (2000).

15 Kosa, J. L., Zdraveski, Z. Z., Currier, S., Marinus, M. G. & Essigmann, J. M. RecN and RecG are required for Escherichia coli survival of Bleomycin-induced damage. *Mutat Res* **554**, 149-157, doi:10.1016/j.mrfmmm.2004.04.011 (2004).

16 Meddows, T. R., Savory, A. P., Grove, J. I., Moore, T. & Lloyd, R. G. RecN protein and transcription factor DksA combine to promote faithful recombinational repair of DNA double-strand breaks. *Mol Microbiol* **57**, 97-110, doi:10.1111/j.1365-2958.2005.04677.x (2005).

17 Meddows, T. R., Savory, A. P. & Lloyd, R. G. RecG helicase promotes DNA double-strand break repair. *Mol Microbiol* **52**, 119-132 (2004).

18 Badrinarayanan, A., Reyes-Lamothe, R., Uphoff, S., Leake, M. C. & Sherratt, D. J. In vivo architecture and action of bacterial structural maintenance of chromosome proteins. *Science* **338**, 528-531, doi:10.1126/science.1227126 (2012).

19 Stohl, E. A. *et al.* Escherichia coli RecX inhibits RecA recombinase and coprotease activities in vitro and in vivo. *J Biol Chem* **278**, 2278-2285, doi:10.1074/jbc.M210496200 (2003).

20 Sommer, S., Boudsocq, F., Devoret, R. & Bailone, A. Specific RecA amino acid changes affect RecA-UmuD'C interaction. *Mol Microbiol* **28**, 281-291 (1998).

21 Sassanfar, M. & Roberts, J. Constitutive and UV-mediated activation of RecA protein: combined effects of recA441 and recF143 mutations and of addition of nucleosides and adenine. *J Bacteriol* **173**, 5869-5875 (1991).
22 Karu, A. E. & Belk, E. D. Induction of E. coli recA protein via recBC and alternate pathways: quantitation by enzyme-linked immunosorbent assay (ELISA). *Mol Gen Genet* **185**, 275-282 (1982).
23 Bell, J. C., Plank, J. L., Dombrowski, C. C. & Kowalczykowski, S. C. Direct imaging of RecA nucleation and growth on single molecules of SSB-coated ssDNA. *Nature* **491**, 274-278, doi:10.1038/nature11598 (2012).
24 Feinstein, E. *et al.* Single-molecule studies of the stringency factors and rates governing the polymerization of RecA on double-stranded DNA. *Nucleic Acids Res* **39**, 3781-3791, doi:10.1093/nar/gkr013 (2011).
25 Chen, Z., Yang, H. & Pavletich, N. P. Mechanism of homologous recombination from the RecA-ssDNA/dsDNA structures. *Nature* **453**, 489-484, doi:10.1038/nature06971 (2008).
26 Story, R. M., Weber, I. T. & Steitz, T. A. The structure of the E. coli recA protein monomer and polymer. *Nature* **355**, 318-325, doi:10.1038/355318a0 (1992).
27 Yu, X., VanLoock, M. S., Yang, S., Reese, J. T. & Egelman, E. H. What is the structure of the RecA-DNA filament? *Current protein & peptide science* **5**, 73-79 (2004).
28 Egelman, E. H. & Stasiak, A. Structure of helical RecA-DNA complexes. Complexes formed in the presence of ATP-gamma-S or ATP. *J Mol Biol* **191**, 677-697 (1986).
29 Brenner, S. L., Zlotnick, A. & Griffith, J. D. RecA protein self-assembly. Multiple discrete aggregation states. *J Mol Biol* **204**, 959-972. (1988).
30 Cox, M. M. Regulation of bacterial RecA protein function. *Critical reviews in biochemistry and molecular biology* **42**, 41-63, doi:10.1080/10409230701260258 (2007).
31 DiCapua, E., Schnarr, M., Ruigrok, R. W., Lindner, P. & Timmins, P. A. Complexes of RecA protein in solution. A study by small angle neutron scattering. *J Mol Biol* **214**, 557-570, doi:10.1016/0022-2836(90)90198-U (1990).
32 Levin-Zaidman, S. *et al.* Ordered intracellular RecA-DNA assemblies: a potential site of in vivo RecA-mediated activities. *Proc Natl Acad Sci U S A* **97**, 6791-6796, doi:10.1073/pnas.090532397 (2000).
33 Renzette, N. & Sandler, S. J. Requirements for ATP binding and hydrolysis in RecA function in Escherichia coli. *Mol Microbiol* **67**, 1347-1359, doi:10.1111/j.1365-2958.2008.06130.x (2008).
34 Kidane, D. & Graumann, P. L. Dynamic formation of RecA filaments at DNA double strand break repair centers in live cells. *The Journal of cell biology* **170**, 357-366, doi:10.1083/jcb.200412090 (2005).